Fall 2018

Bridge deck assessment using visual inspection, ground penetrating radar, portable seismic property analyzer-ultrasonic surface wave, hammer sounding and chain drag

Abdullah Hadi Zaid Alhaj

Department:

BRIDGE DECK ASSESSMENT USING VISUAL INSPECTION, GROUND PENETRATING RADAR, PORTABLE SEISMIC PROPERTY ANALYZER-ULTRASONIC SURFACE WAVE, HAMMER SOUNDING AND CHAIN DRAG

By

ABDULLAH HADI ZAID ALHAJ

A THESIS

Presented to the Faculty of the Graduate School of the

MISSOURI UNIVERSITY OF SCIENCE AND TECHNOLOGY

In Partial Fulfillment of the Requirements for the Degree

MASTER OF SCIENCE

IN

GEOLOGICAL ENGINEERING

2018

Committee

Neil L. Anderson, Advisor

Evgeniy V. Torgashov

J. David Rogers

ABSTRACT

Integrated non-destructive techniques were utilized to assess the condition of a reinforced concrete bridge deck. There were two main objectives accomplished.

The first objective was to assess the integrity of the reinforced concrete bridge deck using four non-destructive techniques, namely visual inspection, ground penetrating radar, portable seismic property analyzer-ultrasonic surface wave, and hammer sounding and chain drag. Visual inspection data were used to identify signs of deterioration on surface of the bridge deck such as cracking, concrete leaching, and reinforcement corrosion. Ground penetrating radar data were used to determine the relative condition of the bridge deck. However, due to the significant differences in depth of the embedded reinforcements, ground penetrating radar data were not useful in terms of assessing the overall condition of the bridge deck. Portable seismic property analyzer-ultrasonic surface wave data were used to determine the concrete quality of the bridge deck by estimating average Young's modulus (elastic modulus). Hammer sounding and chain drag data were used to identify non-delaminated and severe delaminated areas in the bridge deck.

The second objective was to demonstrate the effect of temperature and moisture content changes on ground penetrating radar signal amplitude. Ground penetrating radar signal amplitude variations associated with different weather condition of temperature and moisture changes were evaluated. Ground penetrating radar signal amplitude was increasingly attenuated during low temperature and high moisture content. In contrast, ground penetrating radar signal amplitude was decreasingly attenuated during high temperature low moisture content.

ACKNOWLEDGMENTS

I would like to express my gratitude to my academic advisor Dr. Neil Anderson for his academic and financial support during the period of my master's program and allowing me to participate in multiple funded projects. In addition, I would like to thank my committee members Dr. Evgeniy Torgashov and Dr. David Rogers for accepting to be on my advisory committee. My thanks extended to Dr. Evgeniy Torgashov for his help in providing valuable comments throughout this study. In addition, thanks extend to all staff members and S&T graduate students of the department of geological engineering especially James Hayes, Shishay Kidanu, Hannah Helmick, Shawna Holle, Sharon Lauck, Wendy Albers and Patricia Robertson. I would like to give special thanks to the generous Sheikh Abdullah Bugshan and all Hadhramout Establishment for Human Development (HEHD) scholars for their extremely generous support during my academic program. Special thanks to all my friends inside and outside the states. Finally, my sincere appreciations must go to my kind parents, my brother, my sisters and my precious wife for their love and support throughout my educational journey.

TABLE OF CONTENTS

Page

LIST OF ILLUSTRATIONS

Page

LIST OF TABLES

Page

NOMENCLATURE

Symbol: Description

vi: GPR signal velocity travelling through a medium

εi: dielectric permittivity (dielectric constant) for the medium

c: speed of light in air or free space, which equals 0.3 m/ns or 0.98 ft. /ns

V_S: Shear wave velocity.

V_R: Raleigh wave velocity.

E: Young's modulus.

λ: Poisson's ratio.

ρ: Mass density.

1. INTRODUCTION

Reinforced concrete deterioration is a significant issue and can cause many problems in terms of serviceability and integrity of the bridge decks. Bridge deck assessment is critical and should be cost-effective and reliable to avoid potential of bridge deck failures.

The first objective of this study was to assess the integrity of a reinforced concrete bridge deck by employing multiple non-destructive techniques (NDT) of visual inspection, ground penetrating radar (GPR), portable seismic property analyzer-ultrasonic surface wave (PSPA-USW), and the conventional tools of hammer sounding (HS) and chain drag (CD). The employed multiple techniques were evaluated in order to assess the overall condition of the reinforced concrete bridge deck. Using multiple NDTs is usually recommended to identify different types of deterioration since each technique responds differently to different types of deterioration.

The second objective of this study was to demonstrate the effect of temperature and moisture content changes on GPR signal amplitude. Ground penetrating radar signal amplitude varies with the change of dielectric permittivity of concrete associated with changes on weather conditions of temperature and moisture content.

1.1. BRIDGE DECKS BACKGROUND

The world is more dependent than ever on transportation because of its economic and social importance. Highways and bridges are the most common types of transportation

infrastructure. Countries become more interested in advancing transportation infrastructure including bridges in order to ease commuting. However, bridges are continuously aging and deteriorating due to physical, chemical and bacterial deterioration process. Mitigation of bridge deterioration is critical for transportation decision makers in order to keep the integrity and serviceability of bridge decks and fulfill the safety and security demands since there is a lot of cost involved in implementing and establishing effective techniques to assess the existing bridge decks. Therefore, NDT can be utilized to provide a rapid and cost-effective bridge deck assessment. The acquired NDT data can be interpreted to assess the overall condition of reinforced concrete bridge decks and understand the deterioration process within the bridge deck, which might be used to predict and avoid potential bridge deck failure [1].

1.2. BRIDGE DECK DETERIORATION

Reinforced concrete bridge decks lose their integrity with time passing as a result of deterioration as shown in (Figure 1.1). Bridge deck deterioration is created by multiple physical, chemical and bacterial deterioration processes that cause spalling, reinforcement corrosion, concrete leaching, scaling, etc. as summarized in (Table 1.1). Regular and effective assessment is essential to keep the integrity of bridge decks in order to avoid significant cost of repairing and replacing deteriorated bridge decks. For instance, the repairing and replacing cost of deteriorated U.S. highway bridge decks was estimated by FHWA at approximately $100 billion [2, and 3]. Therefore, understanding the deterioration

process is necessary to select the appropriate non-destructive techniques for bridge deck assessment [2, 3, 4, and 5].

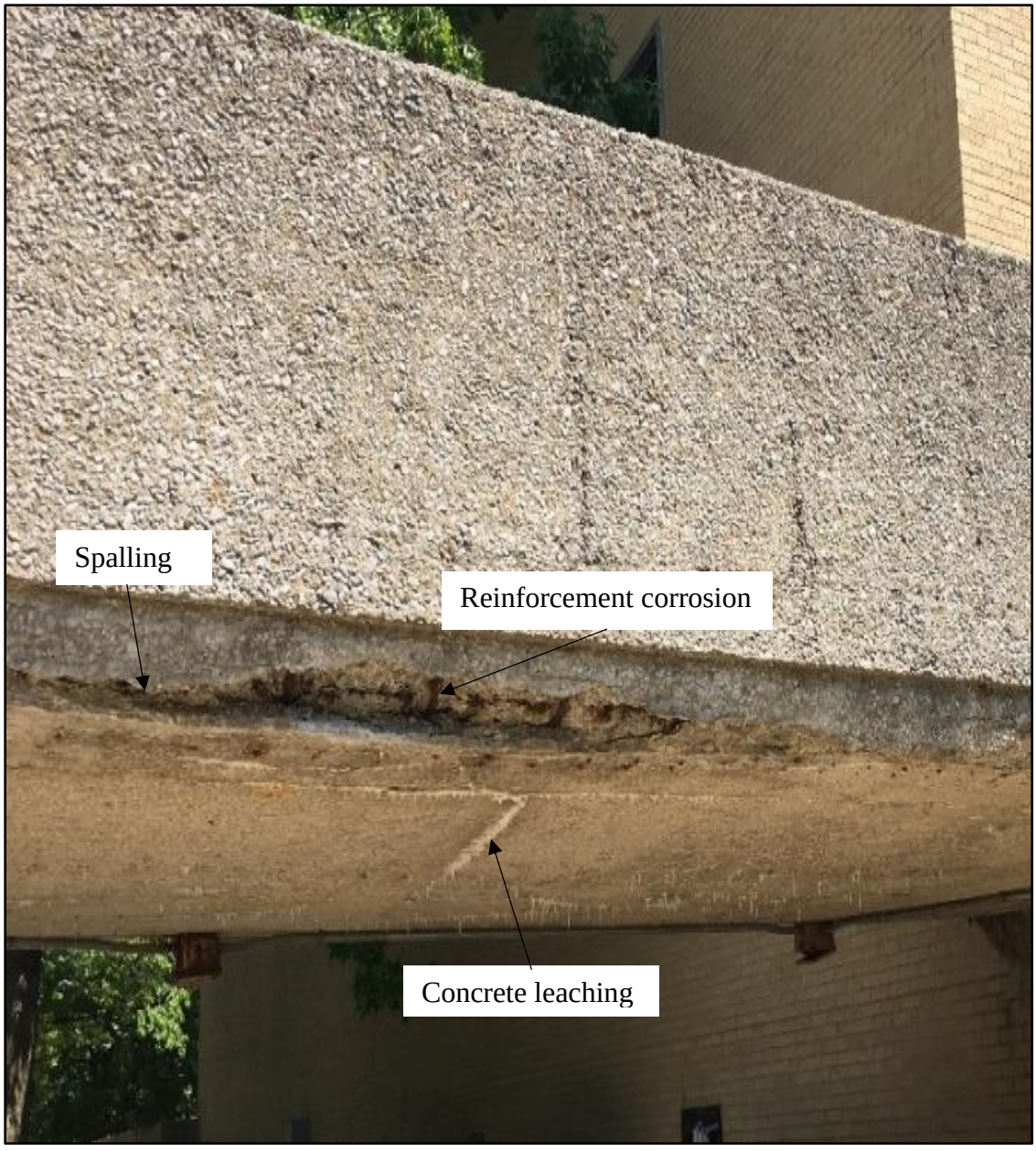

Figure 1.1. Bridge deck deterioration.

Table 1.1. Summary of common problems in reinforced concrete bridge decks [6 and 7].

Defect	Definition	Cause
Spalling	Fragmenting or delaminating of the concrete surface	Internal pressure due to reinforcement corrosion, and/or freeze thaw cycling, and/or Alkali silica reaction, and/or poor construction practices.
Reinforcement corrosion	The rusting of embedded steel rebars, which creates an expansion of steel / concrete interface until the concrete breaks away from the steel rebar creating cracking and spalling	Chloride ions and carbon dioxide (carbonation) reach the rebar through pores and fractures in concrete, lower the pH and destroys the protective film on rebar.
Leaching	The formation of calcium carbonate or calcium sulphate on the surface of the concrete	Occurs due to dissolving water in concrete like calcium hydroxide at crack locations

Table 1.1. Summary of common problems in reinforced concrete bridge decks [6 and 7] (cont.).

Scaling	The loss of cement paste surrounding the coarse aggregates on a concrete surface	Occurs due to freeze and thaw cycling, moisture and/or deicing salts
Cracking	Breaking or fracturing of concrete into parts	Occurs due to tensile forces caused by shrinkage, freeze and thaw cycling, overloading, reinforcement corrosion, and chemical reactions
Honeycombing	The presence of exposed coarse aggregate without enough concrete paste covering the aggregate, causing the presence of small holes	Poorly graded concrete mix , the use of large coarse aggregate, and insufficient vibration at the time of placement
Delamination	Cracks or fracture planes at or just above the level of reinforcement that grow big and can affect the integrity of the structure	reinforcement corrosion , moisture and chloride content in concrete, cracking in concrete surface

1.2.1. Spalling. Spalling is fragmenting or delaminating of the concrete surface as shown in (Figure 1.2). Spalling is caused by internal pressure and cracking due to presence of reinforcement corrosion, and/or freeze thaw cycling, and/or alkali silica reaction, and/or poor construction practices. This problem can be managed by appropriate covering the steel rebar, lowering water to cement ratio or reducing de-icing salt [4, and 6].

Figure 1.2. Bridge deck deterioration shows spalling.

1.2.2. Reinforcement Corrosion. Reinforcement corrosion is the rusting of embedded steel rebars, which creates an expansion of steel and concrete interface until the concrete breaks away from the steel rebar creating cracking and spalling as shown in (Figure 1.3). Reinforcement corrosion is caused by the chloride ions and carbon dioxide (carbonation) reach the rebar through pores and fractures in concrete, lower the pH and

destroys the protective film on rebar [6, and 7]. Reinforcement corrosion can negatively affect the integrity of the bridge deck by enhancing further cracking, delamination or spalling on the concrete structure[1 and 8].

Figure 1.3. Bridge deck deterioration shows reinforcement corrosion.

1.2.3. Leaching. Concrete leaching occurring by dissolving of calcium hydroxide from the matrix of concrete with presence of water as shown in (Figure 1.4). The removal of soluble materials by water seeping cause degradation and lead to durability problems of concrete [9].

Figure 1.4. Bridge deck deterioration shows concrete leaching.

1.2.4. Scaling. Scaling is the loss of cement paste in concrete mix that leads to expose the aggregate as shown in (Figure 1.5). This problem occurs due to freeze and thaw cycling, moisture and/or deicing salts in concrete [6]. Scaling happens due to the hydraulic pressure of freezing water in the concrete, which exceeds the tensile strength of concrete [10].

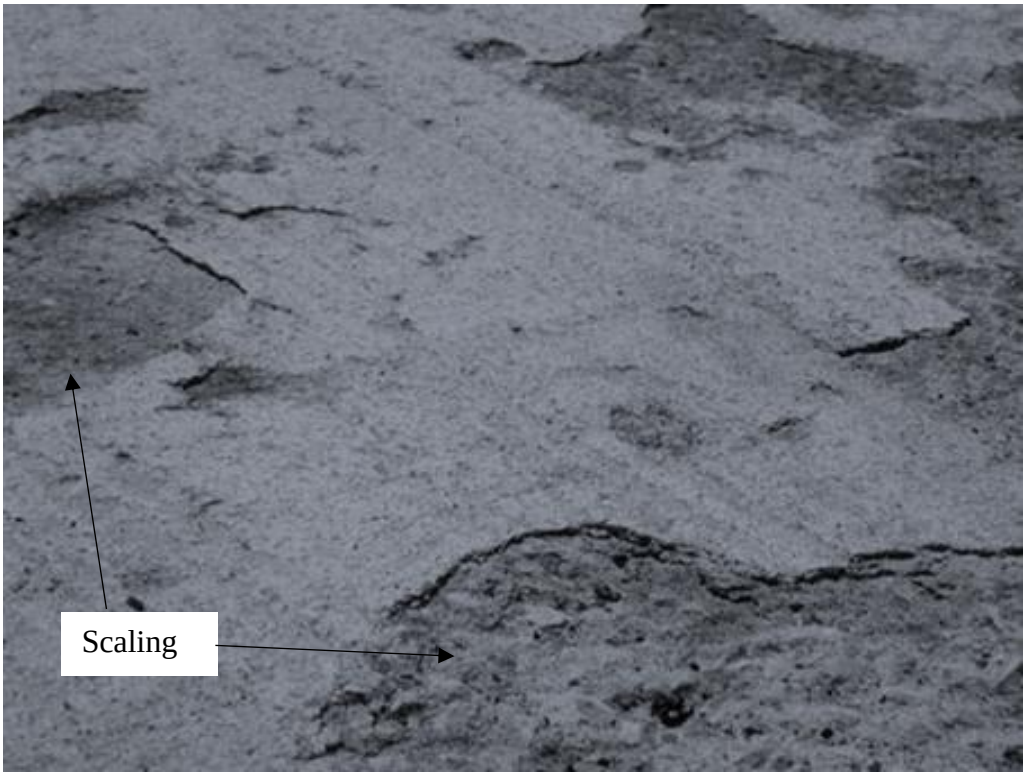

Figure 1.5. Bridge deck deterioration shows concrete scaling.

1.2.5. Cracking. Cracking is breaking or fracturing of concrete bridge deck into small or large parts as shown in (Figure 1.6). It occurs due to tensile forces caused by shrinkage, freeze and thaw cycling, overloading, reinforcement corrosion, and chemical reactions in the concrete bridge deck [1, and 6]. Cracking cause a loss of bond between the concrete and the embedded reinforcements. It also enhance more reinforcement corrosion by allowing chemicals and water to infiltrate into the internal structure of concrete [7]. The progressive reinforcement corrosion can promote further cracking along the concrete structure [4].

Figure 1.6. Bridge deck deterioration shows cracking.

1.2.6. Honeycombing. Honeycombing is the presence of exposed coarse aggregate without enough concrete paste covering the aggregate, causing the presence of small holes as shown in (Figure 1.7). These holes or voids on the surface of concrete are caused by the poorly graded concrete mix, the use of large coarse aggregate, and insufficient vibration at the time of placement after concrete is been poured [6].

Figure 1.7. Bridge deck deterioration shows honeycombing [11].

1.2.7. Delamination. Delamination is internal cracks or fracture planes at or just above the level of reinforcement that grow big and can affect the integrity of the concrete structure as shown in (Figure 1.8).Delamination is caused by reinforcement corrosion, cracking, and moisture and chloride content in concrete [6]. When the embedded reinforcement corrodes, it expands. Such expansion may create a crack or subsurface fracture plane in the concrete at or just above the level of the reinforcement [6]. Delamination is not visible on the concrete surface; however, if repairs are not made in a timely fashion, the delamination progresses to open spalls and eventually affect the integrity of the deck [1 and 8].

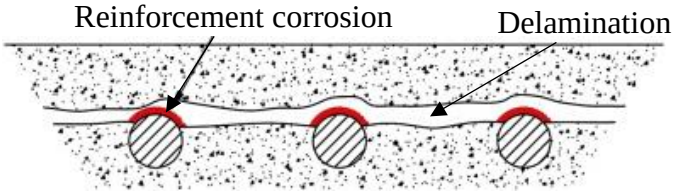

Figure 1.8. Bridge deck deterioration shows delamination [12].

2. AN OVERVIEW OF NON-DESTRUCTIVE TECHNIQUES EMPLOYED FOR BRIDGE DECK ASSESSMENT

Non-destructive techniques, including visual inspection, are considered as effective techniques for bridge deck assessment. Using a single non-destructive technique only provides limited information about the condition of reinforced concrete bridge deck. Therefore, to overcome limitations of using only one individual technique, and constrain results, a complementary approach using several NDTs should be used for effective bridge deck assessment [13 and 14].

The effective reinforced concrete bridge deck assessment should identify different types of deterioration. This can be accomplished by implementing multiple NDTs in order to detect and characterize different types of deterioration such as reinforcement corrosion, concrete leaching and delamination since each technique responds differently to particular type of deterioration as summarized in (Table 2.1). For example, visual inspection can be used to identify signs of deterioration appearing of the surface of the bridge deck such as cracking, spalling and concrete leaching. GPR can be used to determine relative condition of the bridge deck and identify presence of delamination. PSPA-USW can be used to determine concrete quality of the bridge deck by measuring Young's modulus. HS and CD can be used to identify severe deteriorated and non-deteriorated areas on the bridge deck.

There are some factors that should be considered before selecting the appropriate non-destructive technique for bridge deck assessment such as depth of penetration, data resolution, physical property of the target, signal to noise ratio [22] since each NDT has advantages and disadvantages.

Table 2.1. Summary of non-destructive techniques employed for bridge deck assessment.

Method	Uses	Strengths	Limitations
Visual inspection	• An initial technique for bridge deck assessment, which is used to identify signs of deterioration on the surface of bridge deck [15]. • Surface signs of deterioration include cracking, concrete leaching, reinforcement corrosion, etc.	• Accessibility • Rapid data acquisition and no data processing required • Inexpensive compared to the other methods	• Only provide a qualitative interpretation • Constraining and verifying interpretation is required [16] • Slow data acquisition • Doesn't reveal subsurface deterioration and estimate amount of deteriorated concrete need to be repaired or removed[17 and 18] • Qualitative interpretation varies from person to another depending on experience [19]

Table 2.1. Summary of non-destructive techniques employed for bridge deck assessment (cont.).

			• Effective visual inspection might require traffic control [17]
Ground penetrating radar	• Determination of relative condition of bridge deck • Detection of delamination in concrete structure • Image apparent depth to embedded concrete reinforcements	• Portability • Relatively rapid data acquisition and processing [17] • High resolution and reliable results compared to the other methods [17] • Cost-effectiveness compared to the other methods	• Constraining and verifying interpretation is recommended when using as an individual technique • Traffic control maybe required • Doesn't work well in varying depth of concrete reinforcements • Data acquisition, processing and interpretation require experience

Table 2.1. Summary of non-destructive techniques employed for bridge deck assessment (cont.).

		• Quantitative and qualitative interpretation can be obtained • Possible estimation of repair or removal quantities of concrete [17 and 20] • Destructive testing might not be required when using with other integrated NDTs [18].	• Significant changes in temperature and moisture content affect the signal amplitude of GPR • Cannot be used to detect presence of reinforcement corrosion or corrosion rates [1, 20, and 21]

Table 2.1. Summary of non-destructive techniques employed for bridge deck assessment (cont.).

Portable Seismic Property Analyzer-Ultrasonic surface waves	• Strength and quality of concrete by measuring average Young's modulus	• Portability • 1D plot of elastic Young's modulus vs. depth can be obtained • Easy test procedure at relative low cost • Automated data processing • Data is relatively easy to interpret but might need some training	• Slow data acquisition • Used for incipient deterioration • Depth of investigation ≤ 12 (in.) • Traffic control maybe required • Constraining and verifying interpretation is required [16]
Hammer sounding and chain drag	• Detection of no evidence of delamination and severe evidence of delamination	• Accessibility • Portability • Data is used to identify	• Old fashioned technique which is not commonly used • No data processing required

Table 2.1. Summary of non-destructive techniques employed for bridge deck assessment (cont.).

		• non-delaminated and severe delaminated areas on the bridge deck • Inexpensive compared to GPR and PSPA-USW methods	• Relative slow data acquisition • Qualitative interpretation varying from person to another depending on experience • Traffic control maybe required • Constraining and verifying interpretation is required [16]

GPR penetration can image to depth of more than 1 (ft.) compared to the PSPA-USW penetration in which it is only limited to less than 1 (ft.). GPR data can be interpreted both qualitatively and quantitatively whereas visual inspection, HS and CD data only can be interpreted qualitatively depending on inspector experience and level of deterioration.

NDTs should be carefully considered in terms of data acquisition, processing and interpretation to effectively employing these techniques for bridge deck assessment. Multiple NDTs should integrated to constrain and verify results [14].

The acquired NDT data can be interpreted to provide information about the bridge deck condition so that repairs and replacements of deteriorated areas can be planned according to the reliability of the NDT results. The reliable bridge deck assessment can provide valuable information to maintain the bridge deck integrity and avoid potential failure with less time and cost involving [14 and 4].

2.1. VISUAL INSPECTION

The visual inspection or visual evaluation is an initial technique used for bridge deck assessment by observing the general condition of the bridge deck and looking for signs of deterioration appearing on the surface of the bridge deck such as cracking, spalling, patches, and potholes, concrete leaching [15, and 17]. Visual inspection data does not require processing and data is only qualitatively interpreted depending on the inspector experience and level of deterioration.

2.2. GROUND PENETRATING RADAR

GPR is a non-destructive technique that emits pulsed electromagnetic (EM) radiation into a medium as illustrated in (Figure 2.1). The EM radiation or energy is reflected back when it counters an interface in which the material has different dielectric properties (dielectric permittivity and electrical conductivity) compared to the other surrounding materials. The remaining energy propagates deeper into the subsurface and diminishes with depth. The propagation of the EM signal energy of GPR is determined by the dielectric permittivity and electrical conductivity of the material since different materials have different dielectric properties as illustrated in (Table 2.2) .The EM signal speed depends on the dielectric permittivity of material, and the EM signal attenuation depends on the electrical conductivity of material. The GPR receiver records the reflected EM signal as a function of variations on the dielectric properties and measure the amplitude and travel time of the reflected signal. The GPR signal velocity (vi) travelling through a uniform medium can be calculated by using the following Equation 1 [23]:

$$vi = \frac{c}{\sqrt{\varepsilon\ i}} \qquad (1)$$

Where: " ε i" is the dielectric permittivity (dielectric constant) for the medium and "c" is the speed of light in air or free space, which equals 0.3 m/ns or 0.98 ft. /ns.

GPR method is widely used to determine the relative condition of reinforced bridge deck. GPR can image the apparent depth to the top of embedded concrete reinforcements and detect possible presence of delimitation within concrete structure of the bridge deck. GPR data can be interpreted qualitatively and quantitatively.

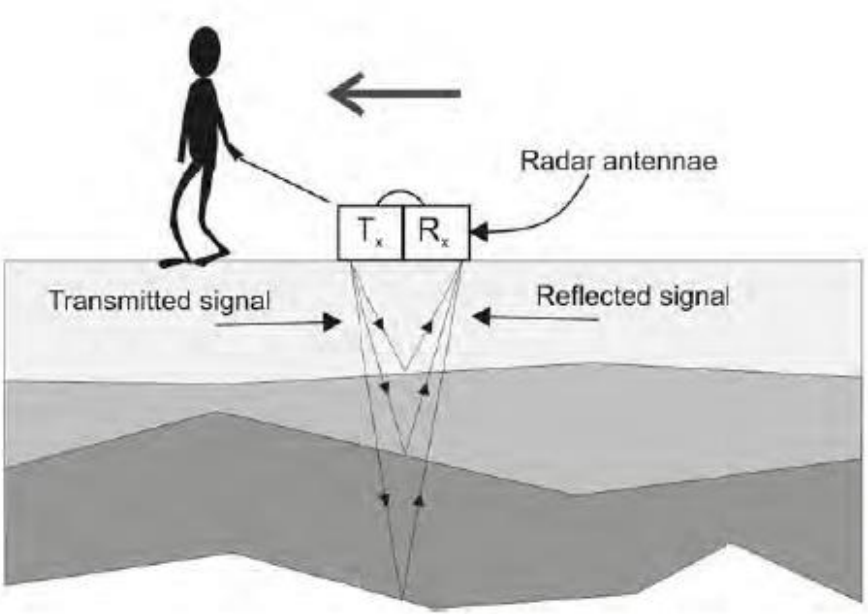

Figure 2.1. GPR operating principle [24].

Table 2.2. Electromagnetic properties of earth materials [1, and 25].

Material	Dielectric permittivity	Conductivity	Velocity, (m/ns)	Attenuation, (dB/m)
Air	1	0	0.3	0
Distilled Water	80	0.001	0.033	0.002
Fresh Water	80	0.5	0.033	0.1
Sea Water	80	3,000	0.01	1,000
Dry Sand	3-5	0.01	0.15	0.01
Wet Sand	20-30	0.1-1	0.06	0.03-0.3
Limestone	4-8	0.5-2	0.12	0.4-1
Shales	5-15	1-100	0.09	1-100

Table 2.2. Electromagnetic properties of earth materials [1, and 25] (cont.).

Silts	5-30	1-100	0.07	1-100
Clays	5-40	2-1,000	0.06	1-300
Granite	4-6	0.01-1	0.13	0.01-1
Dry Salt	5-6	0.01-1	0.13	0.01-1
Ice	3-4	0.01	0.16	0.01

Qualitative GPR interpretation is conducted by visual analysis of the GPR data (travel time and magnitude) whereas, the quantitative GPR interpretation is conducted by post processing of the GPR data (travel time and magnitude) using processing software package and then converting the GPR data into a plan view map to show the variations of concrete condition along the reinforced concrete bridge deck [20].

A given example of GPR scans are shown in (Figures 2.2 and 2.3) which illustrate a vertical scale of apparent depth (in.) and a horizontal scale of distance (ft.). The GPR scans show areas of concrete delamination and varying apparent depth to the top of embedded concrete reinforcements. Therefore, due to varying apparent depth of reinforcements, GPR data is not useful to assess bridge deck condition in this study. Typically, bridge deck assessment using GPR is determined by the relative concrete condition with consistent embedded depth of reinforcements. Where area of good concrete condition or no evidence of deterioration is associated with shallow apparent depth of reinforcements and/or stronger hyperbolic reflections (bright reflections), while area of evidence of deterioration is associated with deep apparent depth of reinforcements and/or weaker hyperbolic reflections (blurred reflections).

The quantitative interpretation is determined by the amplitude ranges of reflections [13, and 20]. The concrete condition threshold of GPR data is visually evaluated by "identifying amplitude ranges" for areas of no evidence of deterioration and areas of severe evidence of deterioration on the bridge deck where highest amplitude indicates area of good concrete condition or no evidence of deterioration and lowest amplitude indicates area of severe concrete condition or severe evidence of deterioration. Eventually, a plan view map should be generated to demonstrate the relative concrete condition according to amplitude variations along the reinforced concrete bridge deck.

A given example of GPR normalized amplitude variations map is shown in (Figure 2.4) illustrating a relative concrete condition along the bridge deck. Where highest amplitude range indicates of good concrete condition (no evidence of deterioration) and lowest amplitude range indicates of severe concrete condition (severe evidence of deterioration).

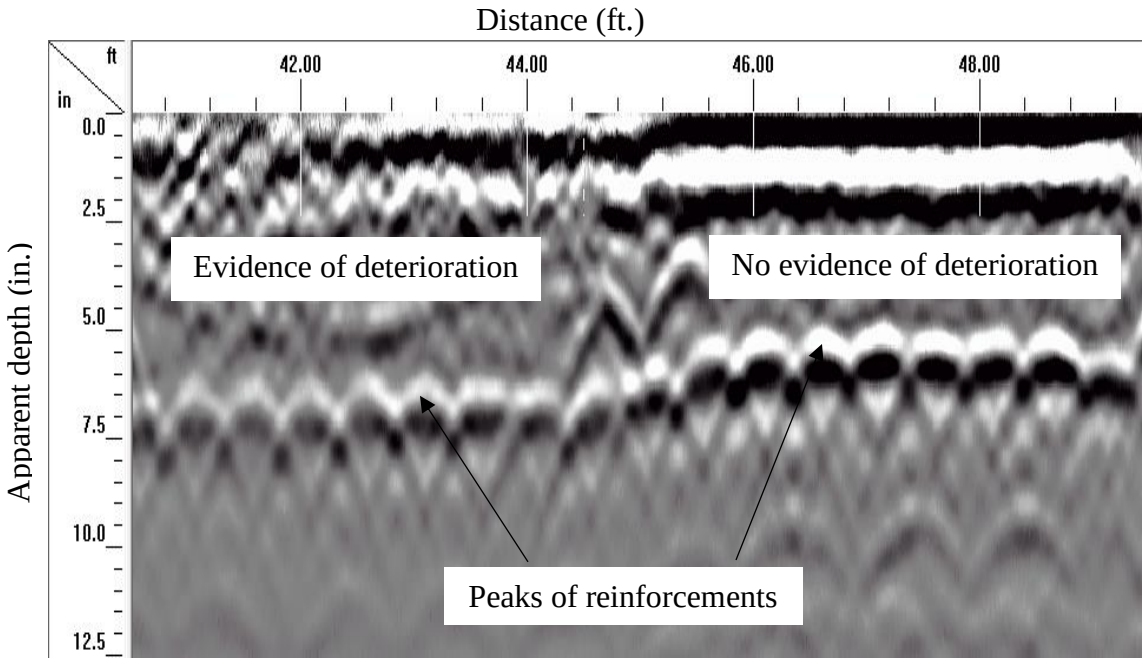

Figure 2.2. Example of GPR data shows reflections from top of embedded reinforcements.

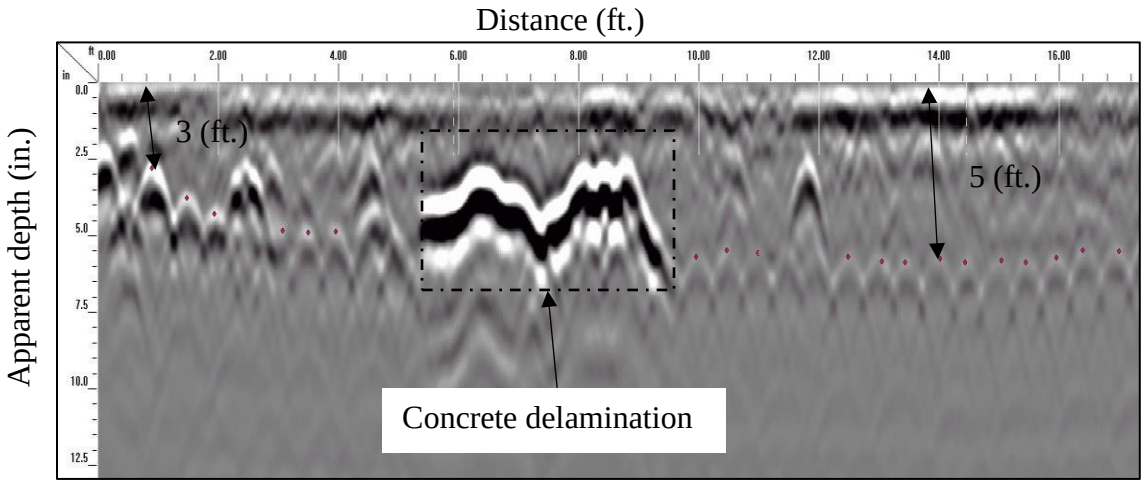

Figure 2.3. Example of GPR data shows delamination and varying depth to top of embedded reinforcements.

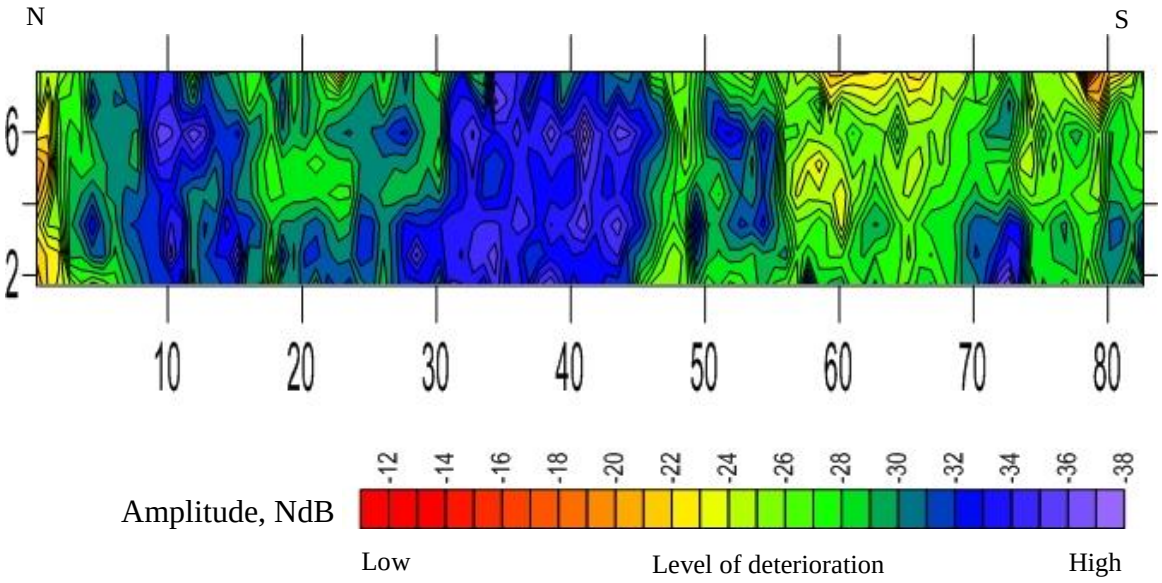

Figure 2.4. Example of GPR amplitude variations map shows level of deterioration on bridge deck.

2.3. PORTABLE SEISMIC PROPERTY ANALYZER-ULTRASONIC SURFACE WAVE

Ultrasonic surface wave (USW) applied in portable seismic property analyzer (PSPA) is known as PSPA-USW. PSPA-USW is a non-destructive technique used to test concrete quality by estimating the average Young's modulus (elastic modulus) of paved

asphalt and/or concrete [17, 25, 26, 27 and 28] as illustrating in (Figure 2.5). The PSPA-USW device components include an acoustic source, two far and near transducers, and electronic box connected to a laptop computer to display and record the data as shown in (Figure 2.6).

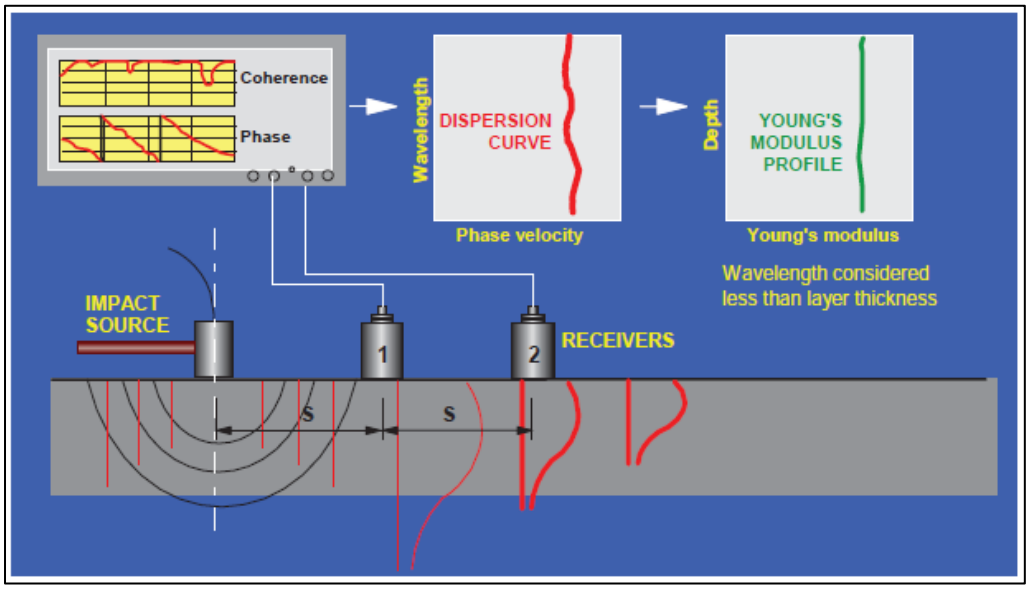

Figure 2.5. PSPA-USW principle [1].

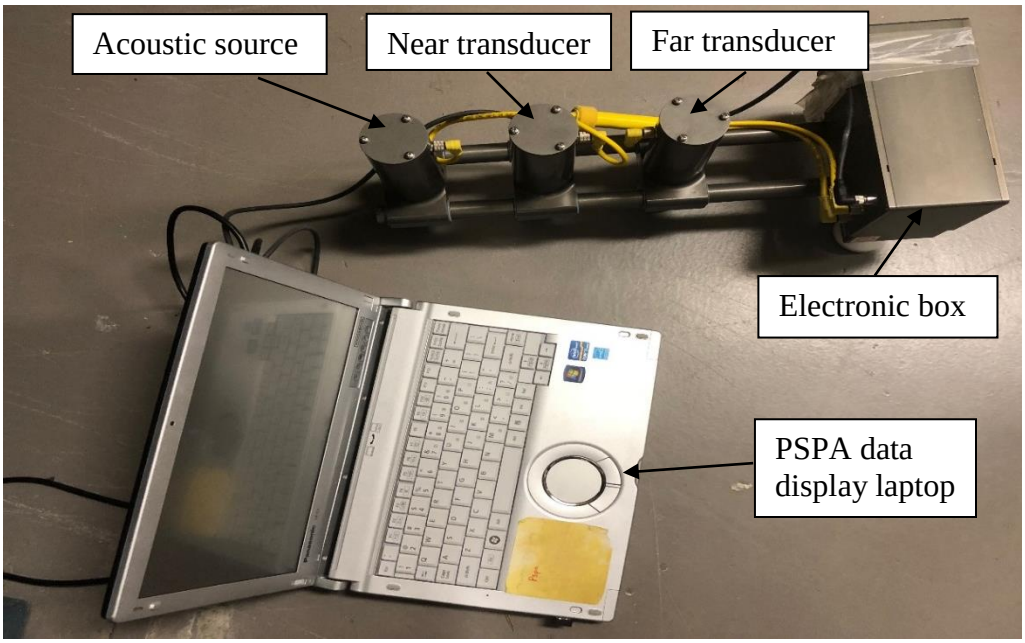

Figure 2.6. Portable seismic property analyzer (PSPA).

PSPA-USW principle is simply using the conversion equation and the computation of average Young's modulus (E). The conversion equation is used to calculate shear wave velocity (VS) from Rayleigh wave velocity (VR) as in Equation 2 [28]:

$$VS = VR\,(1.13 - 0.16\lambda) \quad (2)$$

The computation equation is used to calculate average Young's modulus (E) as in Equation 3 [28]:

$$E = 2\,(\rho)\,VS\,2\,(1 + \lambda) \quad (3)$$

Where: λ = Poisson's ratio, ρ = Mass density.

PSPA-USW measures phase velocities of Rayleigh waves at each test locations and transforms phase velocity at each test location into a 1D plot of Young's modulus [8,28, and 29]. PSPA-USW calculates the average elastic Young's modulus of concrete bridge deck of the uniform materials over the depth range of 2 in. to ~ 7.5 in. based on below Equation 4 [28]:

$$E = 2\rho\,[(1.13-0.16\lambda)\,V_R]^{2}(1+\lambda) \quad (4)$$

It is usually recommended to acquire PSPA-USW data point at least four times at each test location for a 95% confidence. The 1D plot of Young's modulus (ksi) vs concrete depth (in.) shows the strength of concrete material as shown in (Figure 2.7).

According to literature [8,20, and 26], a rating scale of Young's modulus for concrete quality divide concrete condition into four categories as illustrated in (Table 2.3) : "Good concrete condition", "Fair concrete condition", "Poor concrete condition", "Severe concrete condition"; where good concrete condition indicates average Young's modulus greater or equal to 5000 (ksi), fair concrete condition indicates average Young's modulus

in range of 5000-4500 (ksi), poor concrete condition indicates average Young's modulus in range of 4500-4000 (ksi), severely deteriorated concrete condition indicates average Young's modulus less or equal to 3500 (ksi).

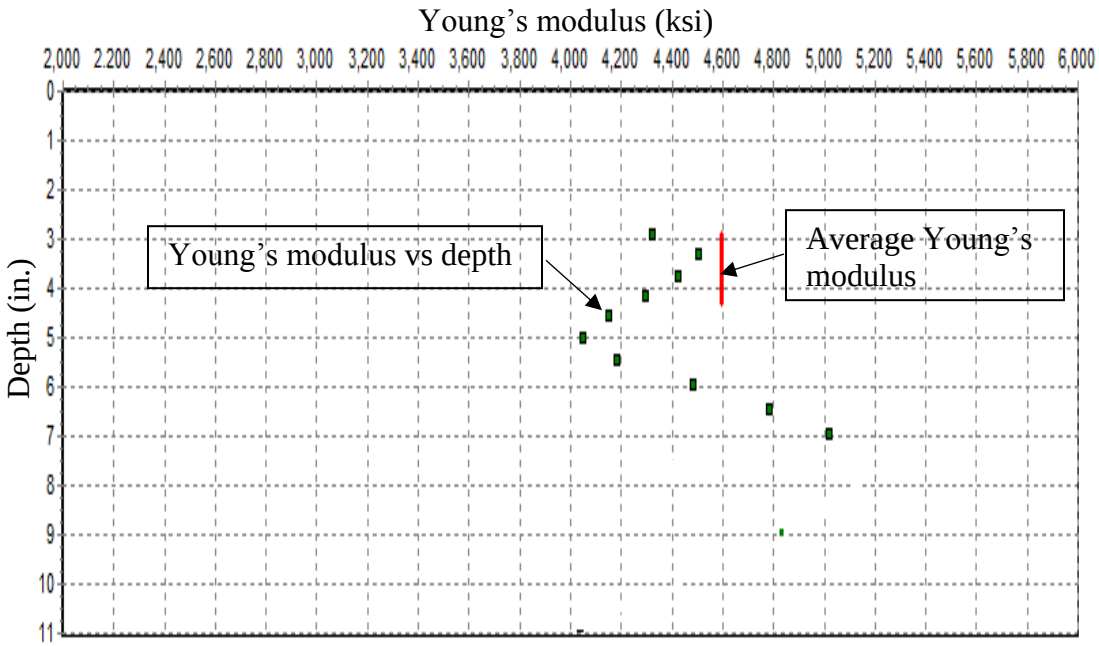

Figure 2.7. 1D plot of Young's modulus (ksi) vs. depth (in.)

Table 2.3. Typical values of elastic modulus for concrete bridge deck [26].

Concrete quality	Elastic modulus (ksi)
Good	≥ 5000
Fair	4500-5000
Poor	4000-4500
Severely deteriorated	≤ 3000

2.4. HAMMER SOUNDING AND CHAIN DRAG

Hammer sounding and chain drag are conventional techniques that can be used for bridge deck assessment as shown in (Figure 2.8.) and (Figure 2.9.) respectively. These techniques are mainly used to detect non-delaminated and severe delaminated areas on the bridge deck. Chain drag is limited to horizontal surfaces, and hammer sounding can be used for a wider range of surfaces [30]. Historically, these techniques were used to be the most common techniques employed by state transportation departments and other bridge deck inspectors to detect the delamination in concrete structure. The objective of these techniques is to detect area of the deck where the sound from dragging the chain or hitting with a hammer changes from a clear solid sound (no delamination) to a somewhat mute or hollow sound (delamination) [1, 6 and 8]. Hammer sounding and chain drag data are qualitatively interpreted and data interpretation varies depending on the experience of the inspector and the level of deterioration.

Using hammer sounding and chain drag for bridge deck assessment should follow standard practice [3 and 29]. The standard, ASTM D4580-12, includes setup of the geometry along particular areas or the whole area of the bridge deck, and then tapping the hammer or dragging the chain over the concrete bridge deck. Hollow or solid sound can be heard during implementing these methods, where hollow sound is indicative of delamination and solid sound is indicative of non-delamination [22 and 24]. Eventually, the delaminated areas are mapped along the bridge deck. Hammer sounding and chain drag can provide inexpensive and rapid data that can be used for bridge deck assessment. However, the data interpretation is subjective or qualitative [20, 31, and 19].

Figure 2.8. Hammer sounding [1].

Figure 2.9. Chain drag [1].

3. THE EFFECT OF TEMPERATURE AND MOISTURE CONTENT CHANGES ON GROUND PENETRATING RADAR SIGNAL AMPLITUDE

3.1. GROUND PENETRATING RADAR SIGNAL

The increase of saline moisture cause an increase on the dielectric permittivity and electrical conductivity of concrete material of the bridge deck. Therefore, the GPR signal amplitude vary with change of dielectric properties of the medium since GPR signal propagation is determined by the dielectric permittivity and electrical conductivity of the subsurface.

GPR signal amplitude highly attenuate when propagating through a high moisture content in concrete due to increasing of dielectric permittivity and electrical conductivity. Moisture content of concrete changes as a result of changes in weather conditions. GPR signal travel time (converted to apparent depth) increases and signal amplitude decreases on deteriorated areas compared to no-deteriorated areas. However, this is not always the case with varying apparent depth of embedded concrete reinforcements [32 and 33].

GPR is used to determine relative condition of reinforced concrete bridge decks in terms deterioration of particular categories; “good concrete condition”, “fair concrete condition”, “poor concrete condition”, and “severe concrete condition” [2, 34, 35 and 36].

3.2. TEMPERATURE AND MOISTURE CHANGES

The decrease of moisture content cause dryness of concrete [37].The analysis of the GPR signal amplitude is used to characterize the moisture conditions of concrete where deteriorated concrete condition is associated with increase of moisture content [37]. The presence of high moisture content increases the dielectric permittivity and conductivity of

the concrete. However, temperature changes have less effect on a dry concrete in which dielectric permittivity of concrete is decreasing and more effect on a saturated concrete in which electrical conductivity is increasing [31].

4. STUDY SITE

This study was conducted on a reinforcing concrete bridge deck locating at Missouri University of Science and Technology campus as shown in (Figure 4.1). The description of the bridge deck is summarized in (Table 4.1).A sketch of the bridge deck is showing in (Figure 4.2) and concrete reinforcements cross sections are showing in (Figure 4.3).

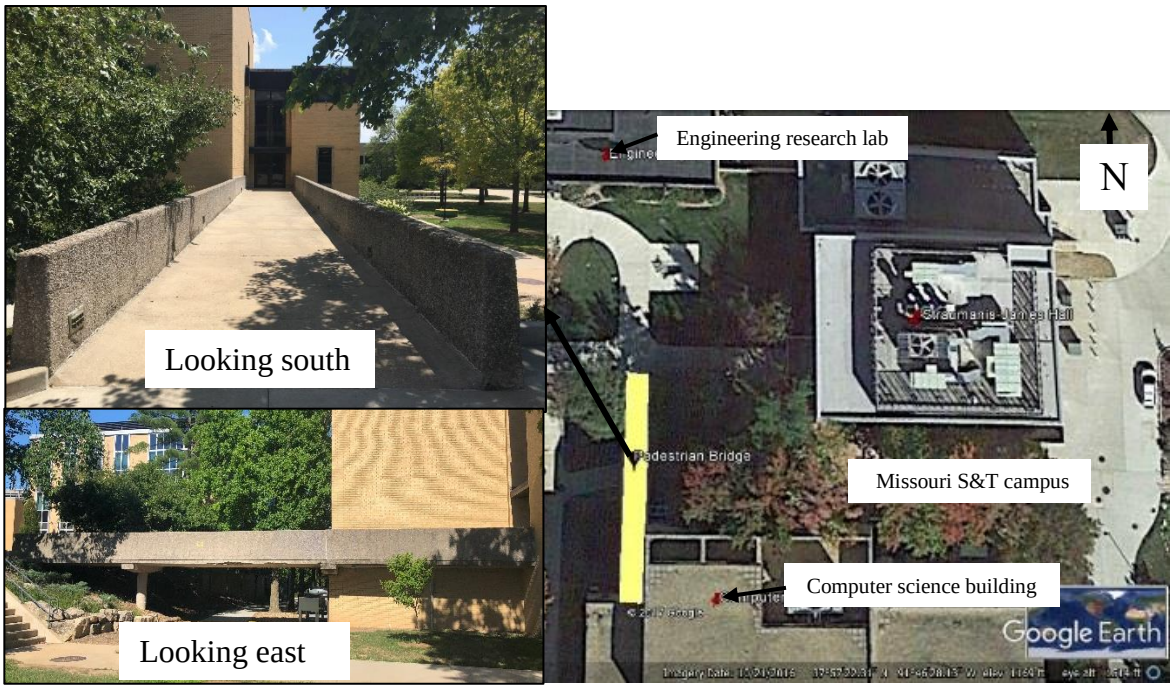

Figure 4.1. Bridge deck (courtesy to Google Earth Pro).

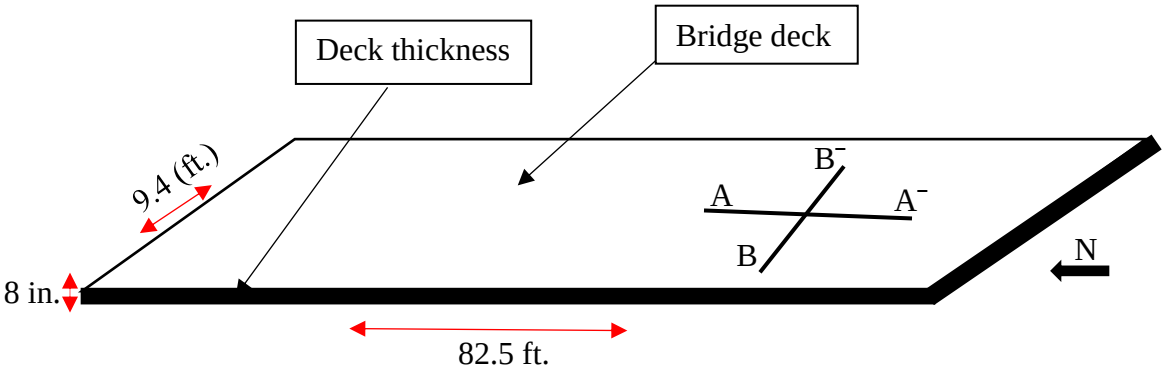

Figure 4.2. Sketch of the bridge deck.

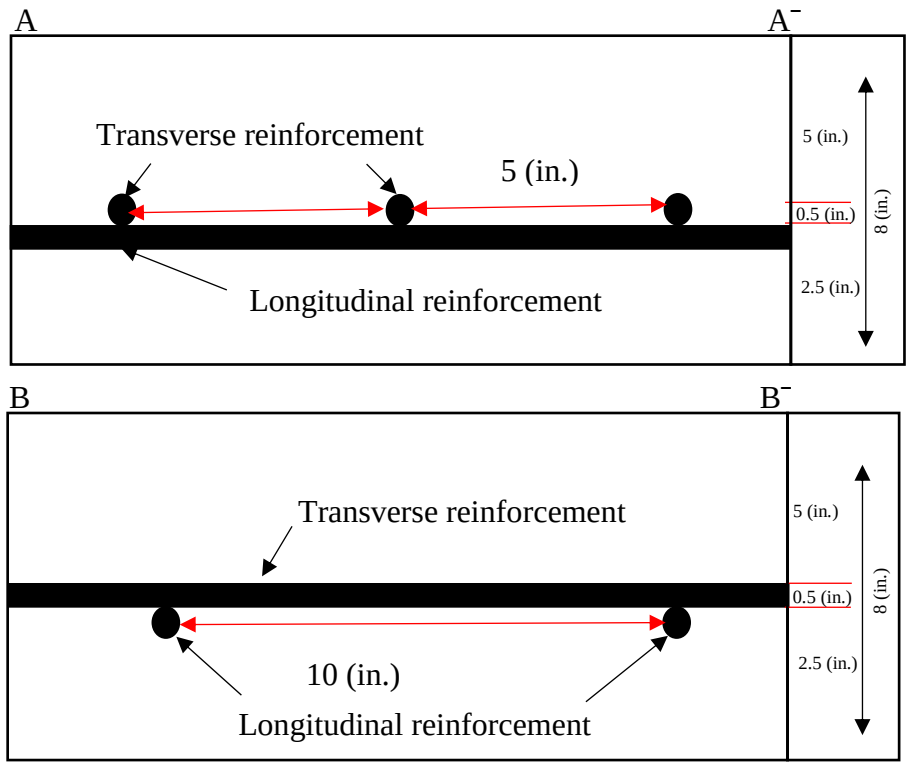

Figure 4.3. Longitudinal (A A⁻) and transverse (B B⁻) cross sections of the bridge deck showing reinforcement details.

Table 4.1. Bridge deck description.

Location	Latitude: 37°57'22.02"N Longitude: 91°46'28.22"W
City-State	Rolla-Missouri
County	Phelps
Year of construction	Unknown
Type of bridge	Pedestrian reinforced concrete bridge
Structure length	83 ft.
Width	10 ft.
Deck material	Portland cement concrete
Thickness	8 in.
Wearing surface	Cracking, leaching and reinforcement corrosion
Orientation of top of reinforcement	West to east
Designed depth to top traverse of reinforcements	4-5 in.
Other Information	According to data interpretation, The bridge deck assessment shows evidence of deterioration

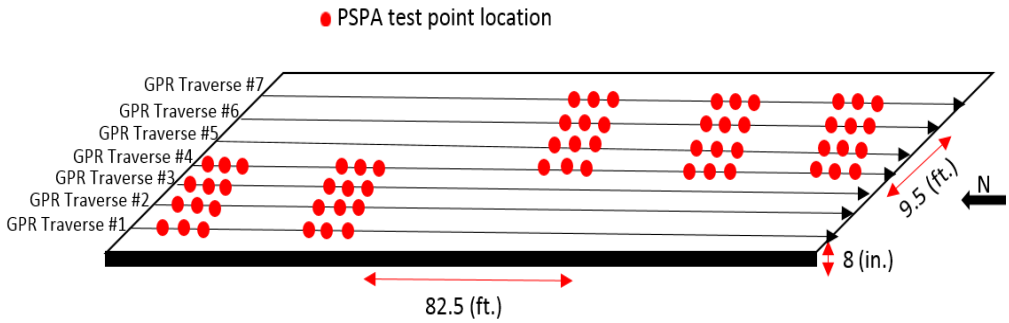

Figure 4.4. Plan view map depicting GPR traverses and PSPA test locations on the bridge deck (not to scale).

5. DATA ACQUISITION AND PROCESSING

5.1. VISUAL INSPECTION

Visual inspection data were acquired by observing signs of deterioration on surface of the reinforced concrete bridge deck as summarized in (Table 5.1). Visual inspection data included signs of deterioration on top and bottom surface of the reinforced concrete bridge deck such as spalling, reinforcement corrosion, cracking and concrete leaching as shown in (Figures 5.1, 5.2, and 5.3). There was no data processing required and data were mapped on a view map of the bridge deck as shown in (Figure 7.1 discussed later in Section 7) in which data were qualitatively interpreted.

Table 5.1. Summary of bridge deck deterioration observed by visual inspection.

	Concrete patches	Concrete spalling	Concrete potholes	Reinforcement corrosion	Cracking	Concrete leaching
Bridge deck		x		x	x	x

5.2. GROUND PENETRATING RADAR

GPR data were acquired using a GSSI SIR-3000 1.5 GHz ground coupled antenna in monostatic mode (transmitter/receiver housed in a single case), mounted to a push cart as shown in (Figure 5.4). PR data were acquired along 7 parallel traverses of 1.7 (ft.) spacing intervals and each length of about 80 (ft.) along the reinforced concrete bridge deck.

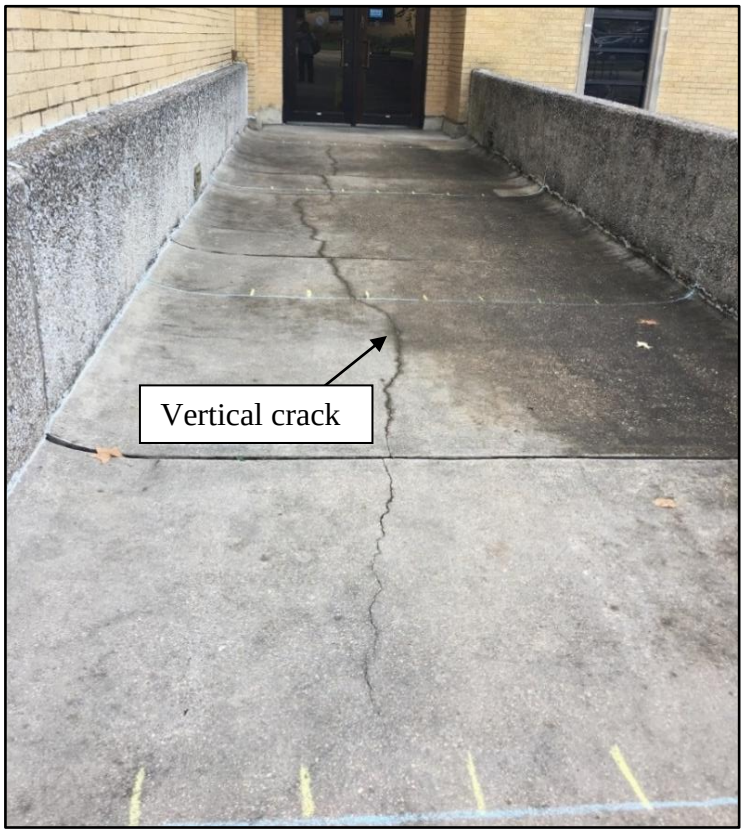

Figure 5.1. Vertical cracking along the top surface of the bridge deck.

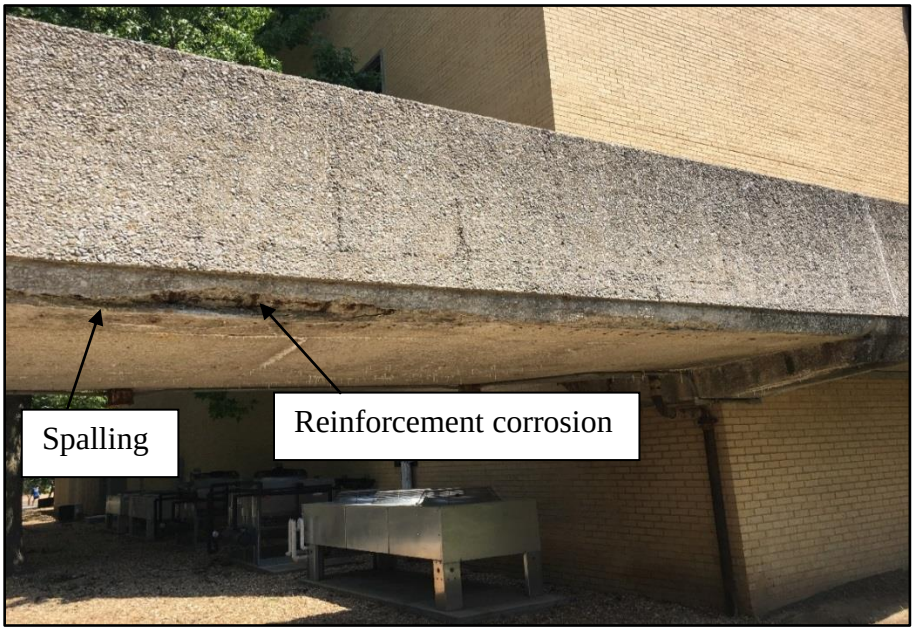

Figure 5.2. Spalling and reinforcement corrosion at the bottom surface of the bridge deck.

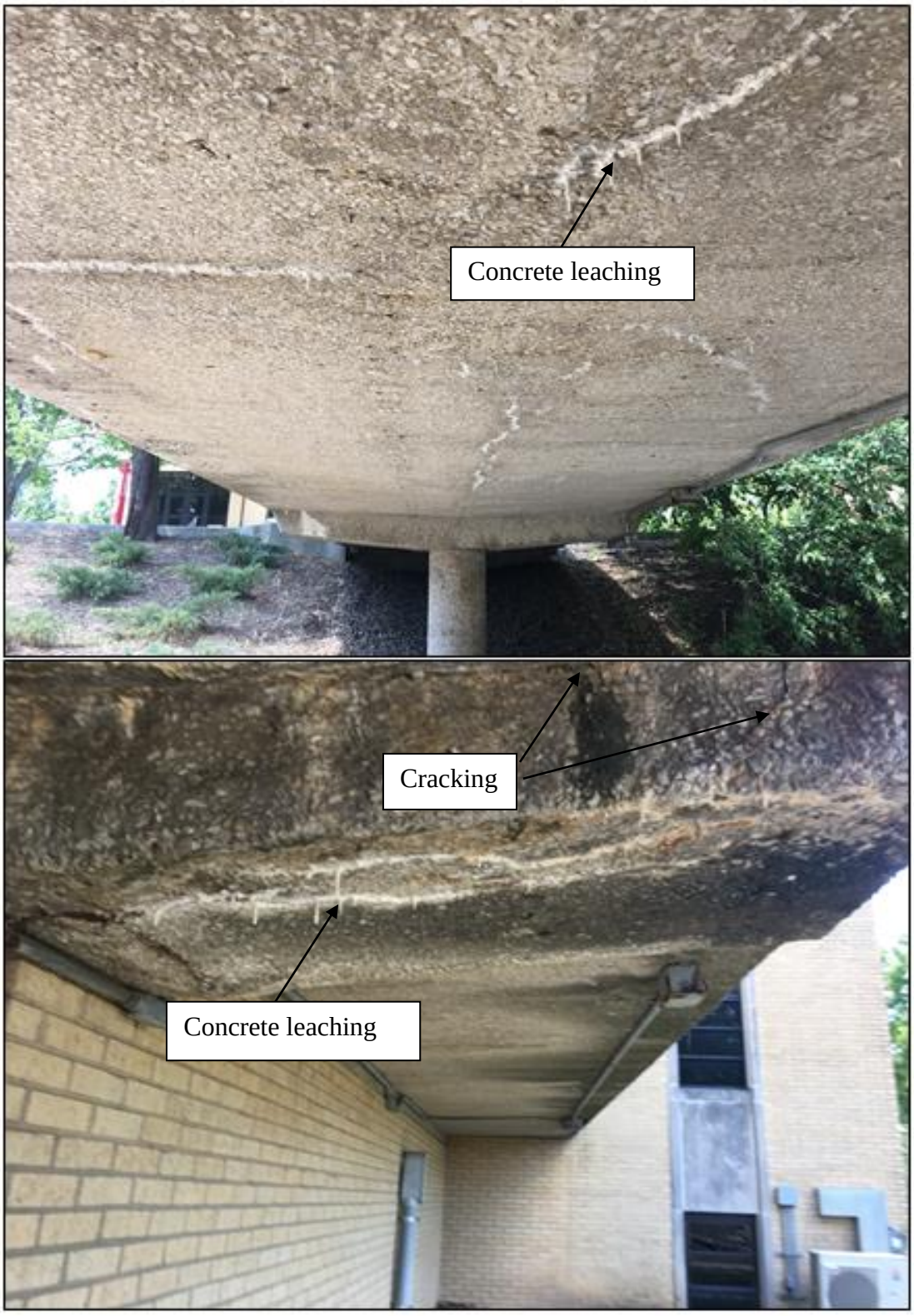

Figure 5.3. Concrete leaching and cracking at the bottom surface of the bridge deck.

The GPR traverses were predetermined and marked with a chalk on the deck surface prior the data acquisition. The GPR traverses' orientation was parallel to traffic flow direction, and longitudinal direction of the bridge beginning from north to south. The intent of GPR surveying was to assess the overall condition of the bridge deck. For effective analysis, the concrete material of the bridge deck was estimated to have the same dielectric constant of 8 (uniform material) in order to assess the concrete condition properly.

After GPR data acquisition, the acquired GPR profiles were patched together and processed by using GSSI RADAN 7 processing software. An example of processed GPR profile is showing in (Figure 5.5). The basic processing steps included time-zero correction, and background removal. The hyperbolic EM reflections were manually picked to calculate the arrival travel time and amplitude of the reflected signals from each reinforcement. Excel spreadsheet was created which includes two-way travel times (in units of nanoseconds, ns) and amplitudes (in units of normalized decibels, NdB). Two-way travel time was converted into apparent depth (in unit of inches, in). Each GPR profile was assigned coordinates (x, y) in the same excel spreadsheet. Finally, two contour maps were generated using Surfer version 10 (by Golden Software) depicting the apparent depth and amplitude variations along the reinforced concrete bridge deck. The amplitude and apparent depth view maps were used to determine the relative concrete conditions according to particular amplitude and apparent depth ranges in which concrete condition is classified into either "good", "fair", "poor", or "severe".

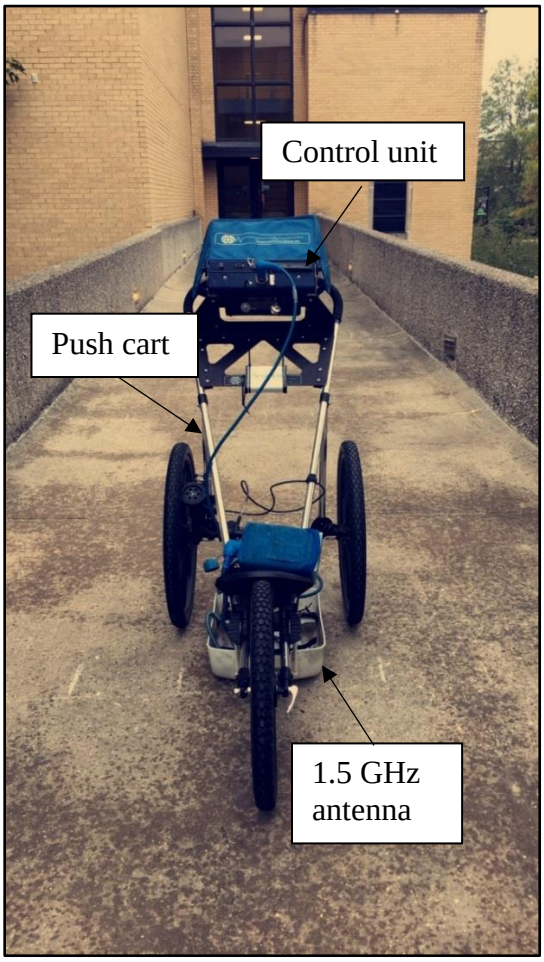

Figure 5.4. GPR data acquisition using a GSSI 1.5 GHz ground coupled antenna.

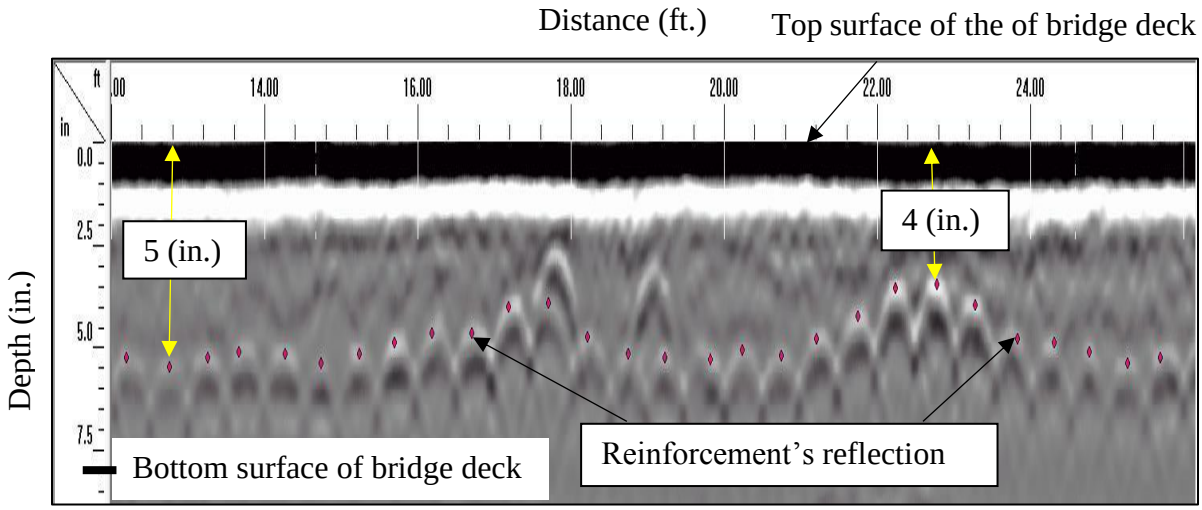

Figure 5.5. GPR profile # 7 shows reflections from varying depth of reinforcements along the bridge deck.

5.3. PORTABLE SEISMIC PROPERTY ANALYZER-ULTRASONIC SURFACE WAVE

The PSPA-USW data were acquired along predetermined sections in which traverses parallel to the GPR traverses. There were five PSPA-USW sections (A, B, C, D, and E) across the reinforced concrete bridge deck. An example of section-A data acquisition is showing in (Figure 5.6). 1D plot of average Young's modulus for each PSPA-USW data point was obtained as shown in (Figure 5.7). PSPA-USW data were automatically processed in situ and there was no need for further post processing. PSPA-USW were transformed from the recorded format in the computer to an excel sheet where each average Young's modulus assigned to a (x, y) coordinate and then imported to Surfer version 10 (by Golden Software) to generate a grid map depicting variations of Young's modulus for each PSPA-USW section.

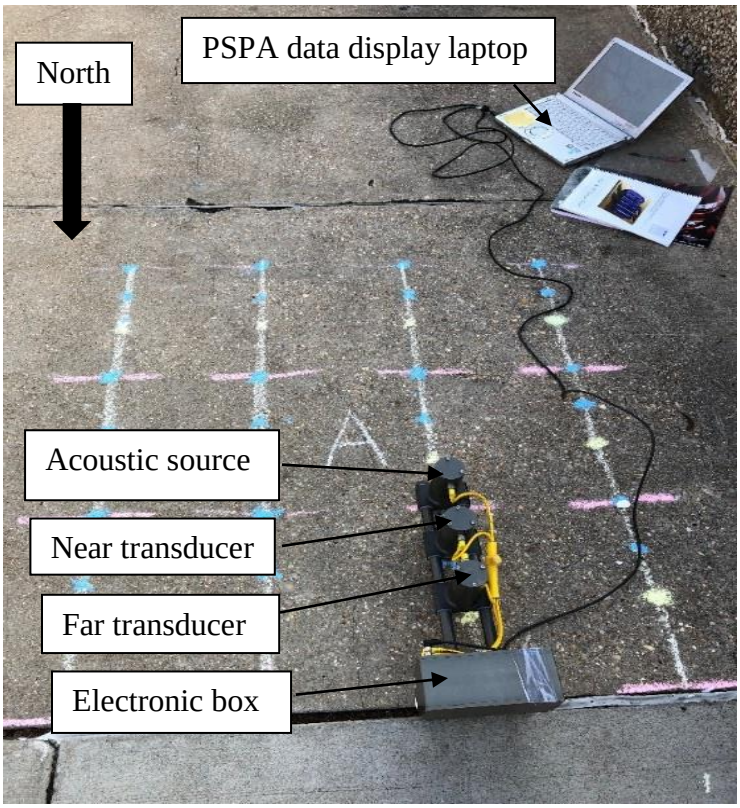

Figure 5.6. PSPA-USW data acquisition.

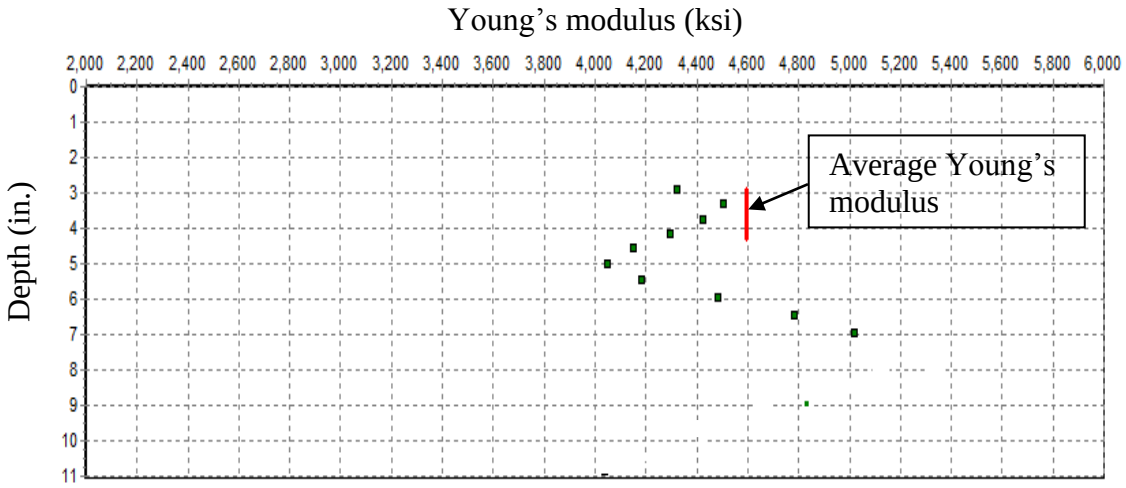

Figure 5.7. Example of PSPA-USW data point depicting average Young's modulus (ksi) vs. depth (in).

PSPA-USW data were acquired at five sections with a grid map of 2 (ft.) by 3 (ft.).The spacing interval was 1 (ft.) and spacing between far and near receiver was set at 4 (in) to get to depth of approximately 2 (in.) to 7.5(in.). Each section location contains 12 PSPA-USW data set. The automatic output of each test location was 1D plot of average Young's modulus vs depth. A contoured map of PSPA-USW data was generated to illustrate the average Young's modulus variations of concrete section in the bridge deck as shown in (Figure 5.8).

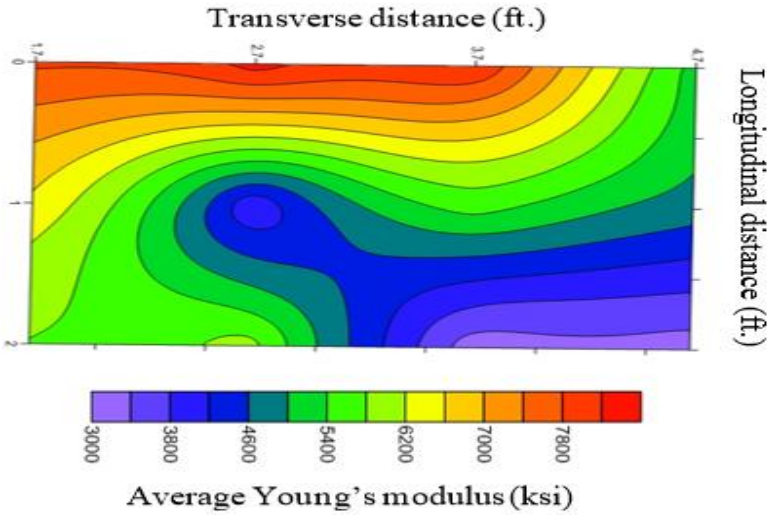

Figure 5.8. Example of contoured map showing variations of average Young's modulus at PSPA-USW section on the bridge deck.

5.4. HAMMER SOUNDING AND CHAIN DRAG

Hammer sounding and chain drag data were acquired along the reinforced concrete bridge deck as shown in (Figures 5.9 and 5.10) respectively. Data were acquired by identifying areas of no delamination (solid sound) and severe delamination (hollow sound). The identified areas were marked with a chalk on the bridge deck as shown in (Figure 5.11). There was no data processing required for this technique. The data were interpreted qualitatively and it could vary from inspector to another depending on the experience and level of deterioration [30 and 38].

Figure 5.9. Hammer sounding.

Figure 5.10. Chain drag.

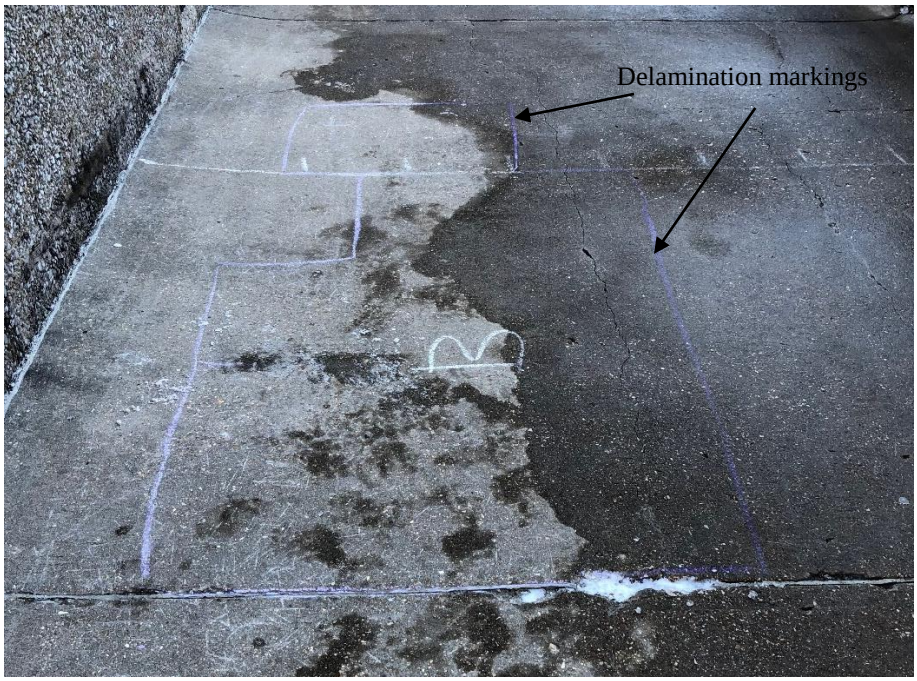

Figure 5.11. Delamination markings.

6. DATA INTERPRETATION AND DISCUSSIONS

6.1. BRIDGE DECK ASSESSMENT

Visual inspection data were qualitatively interpreted to identify signs of deterioration on the top and bottom surface of the reinforced concrete bridge deck as shown in (Figure 6.1). The visual inspection data showed that the central area is the most deteriorated area in the bridge deck. Vertical cracking is passing through the top surface of concrete. Spalling, reinforcement corrosion, and concrete leaching appeared at the bottom surface of the bridge deck. This was an indication that the central area was most likely to be the most deteriorated in the bridge deck.

GPR data was not useful to assess the condition of the reinforced concrete bridge deck due to the significant varying depth to top of embedded concrete reinforcements. However, the author assumed that the apparent depth of reinforcement was consistent in order to correlate the GPR data with the other non-destructive techniques employed in this study for the purpose of constraining and verifying the NDTs results.

The amplitude variations map determined the relative concrete condition of the reinforced concrete bridge deck as shown in (Figure 6.2). The relative concrete condition was divided into four categories: “Good concrete condition” indicated area of no evidence of deterioration, which included amplitude range of 12-18 (NdB); “Fair concrete condition” indicated area of fair evidence of deterioration, which included amplitude range of 18-24 (NdB); “Poor concrete condition” indicated area of evidence of deterioration, which included amplitude range of 24-31 (NdB); “Severe concrete condition” indicated area of severe evidence of deterioration, which includes amplitude range of 31-38 (NdB).

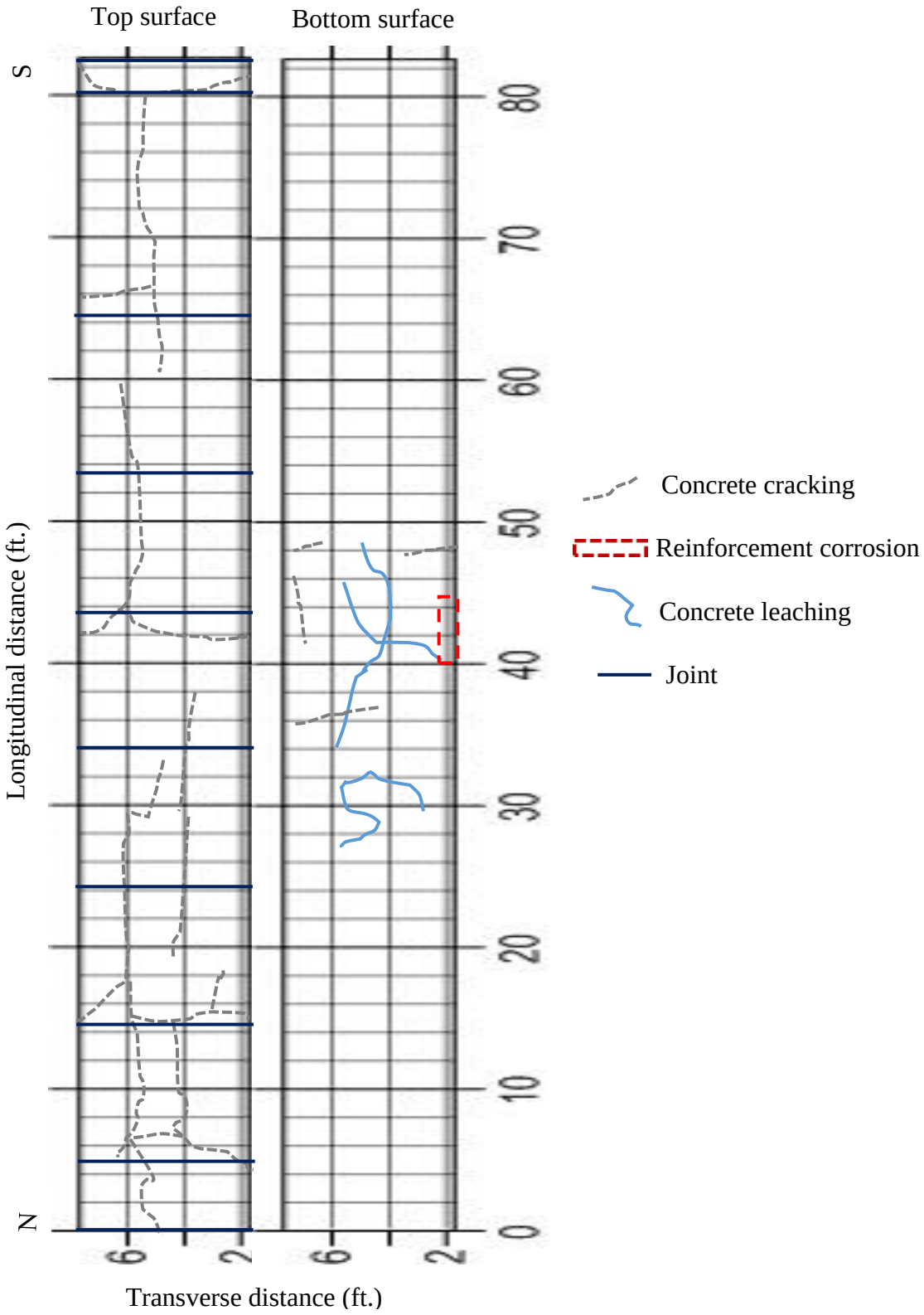

Figure. 6.1. Visual inspection depicting signs of deterioration on top and bottom surface of the bridge deck.

The apparent depth variations map determined the relative concrete condition of the reinforced concrete bridge deck as shown in (Figure 6.3). The relative concrete condition was divided into four categories: “Good concrete condition” indicated area of no evidence of deterioration, which included apparent depth range of 2.8-4.0 (in.); “Fair concrete condition” indicated area of fair evidence of deterioration, which included apparent depth range of 4.0-5.2 (in.); “Poor concrete condition” indicated area of evidence of deterioration, which included apparent depth range of 5.2-6.2 (in.); “Severe concrete condition” indicated area of severe evidence of deterioration, which included apparent depth range of 6.2-7.4 (in.).

The amplitude and apparent depth maps show a good correlation where the area of severe deterioration is mainly located on the center of the bridge deck, while the remaining area of the bridge deck is of approximately moderate to less deterioration.

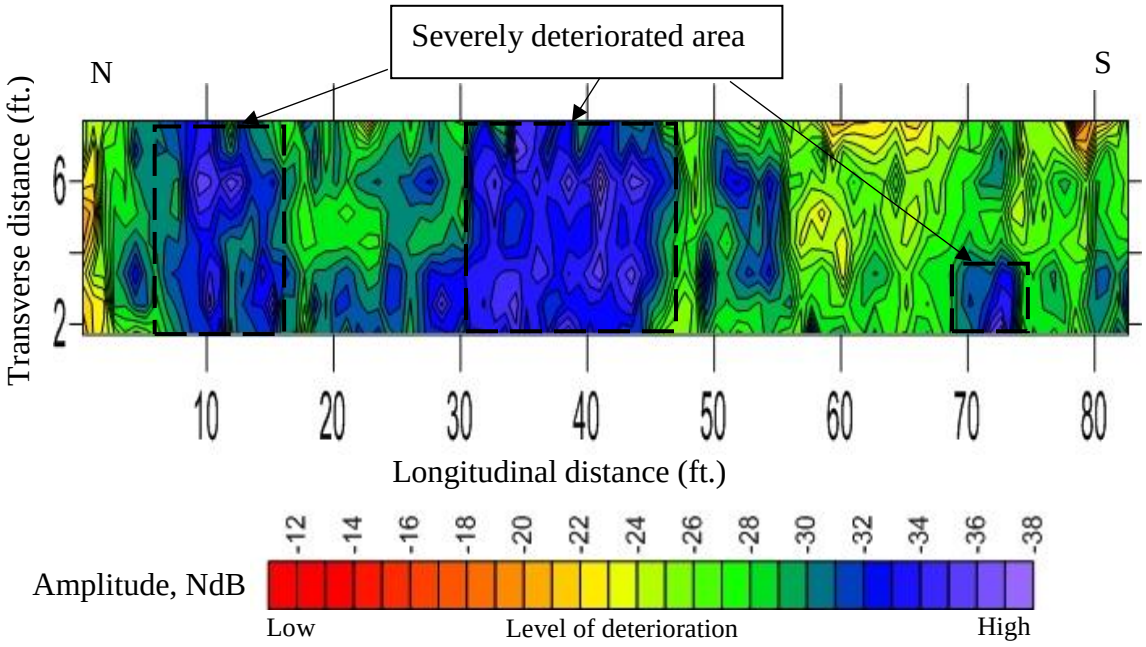

Figure 6.2. GPR amplitude variations map.

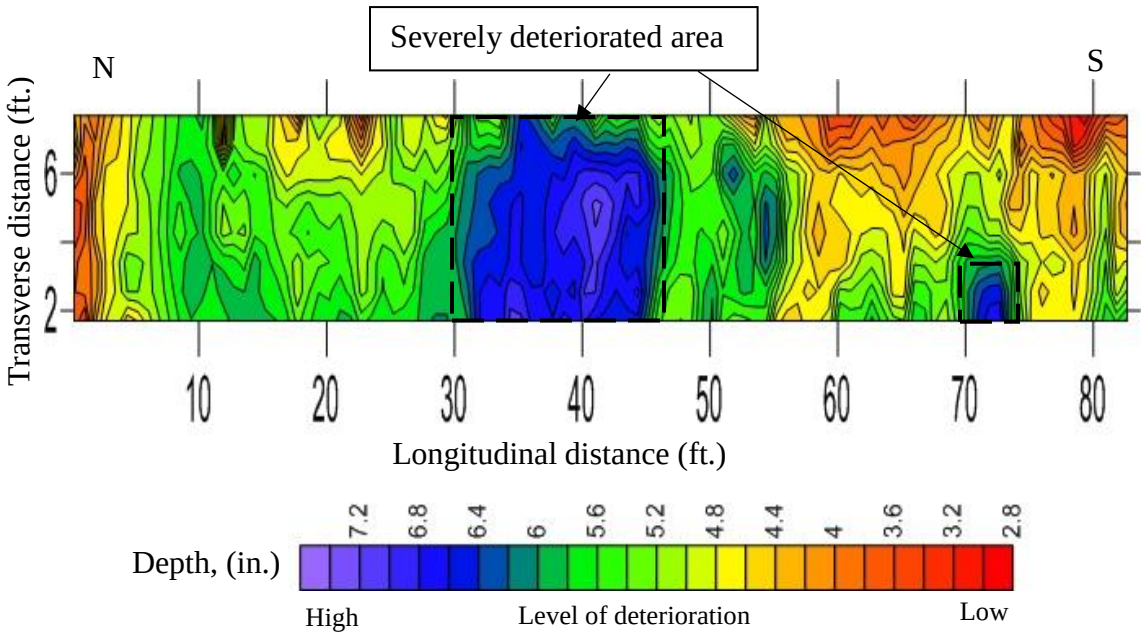

Figure 6.3. GPR apparent depth variations map.

The PSPA-USW data were acquired at five sectional locations (A, B, C, D, and E) on the of the reinforced concrete bridge deck as shown in (Figure 6.4).The PSPA-USW data were interpreted to determine the concrete quality of bridge deck by estimating average Young's modulus. The relative concrete condition was divided according to the average Young's modulus values into four categories: "Good concrete condition" indicated area of average Young's modulus values greater than 5000 (ksi) as in section-A and section-E as shown in (Figures 6.5 and 6.6) respectively; "Fair concrete condition" indicated area of average Young's modulus values range of 5000-4500 (ksi) as in section-C and section-D as shown in (Figures 6.7 and 6.8) respectively. "Poor concrete condition" indicated area of average Young's modulus values range of 4000-3500 (ksi) as in section-B as shown in (Figure 6.9); "Severe concrete condition" indicated area of average Young's modulus values less than 3000 (ksi);

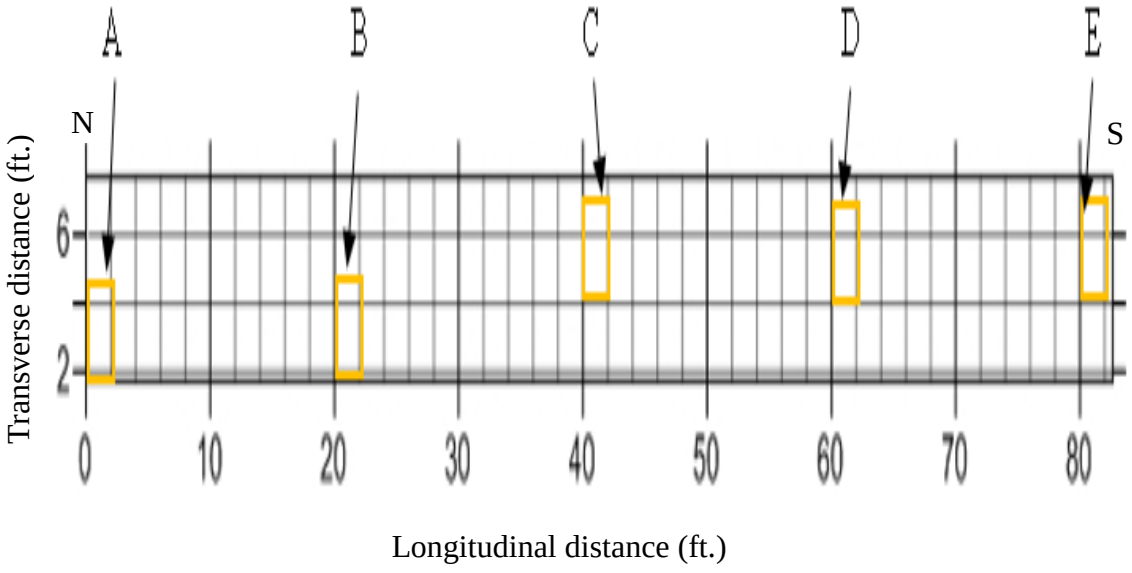

Figure 6.4. PSPA-USW test locations.

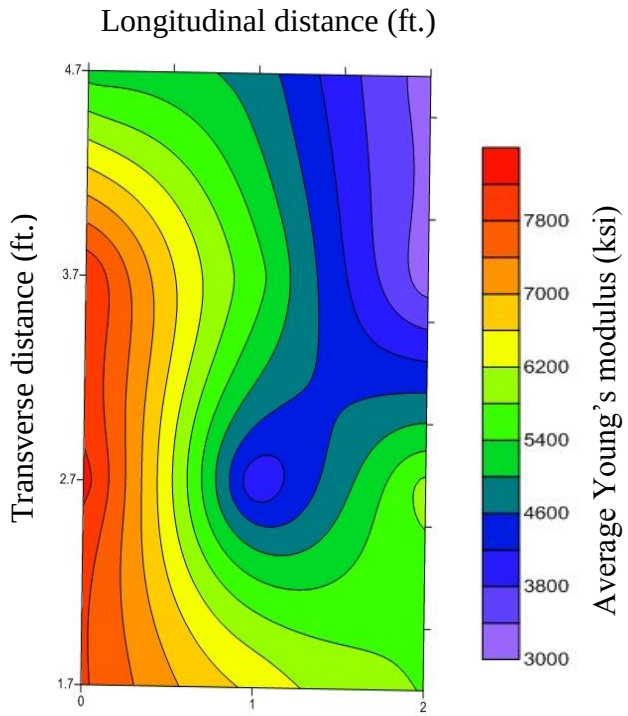

Figure 6.5. Contoured map shows average Young's modulus variations for section (A).

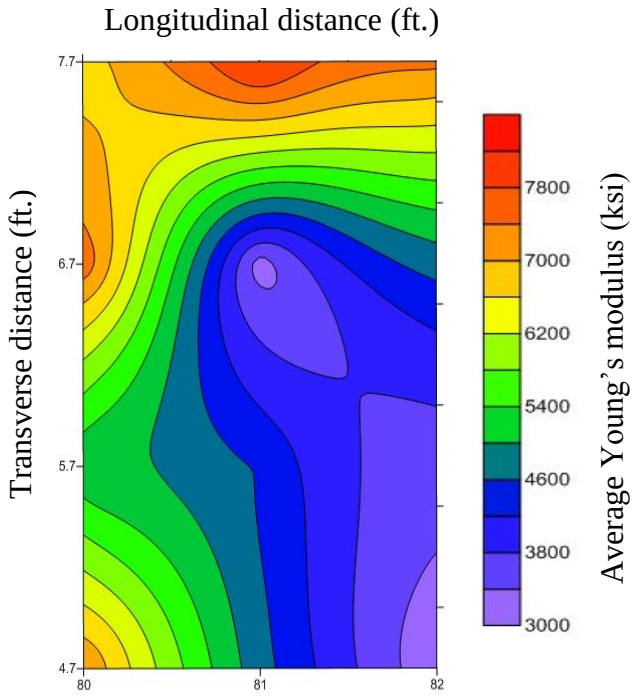

Figure 6.6. Contoured map shows average Young's modulus variations for section (E).

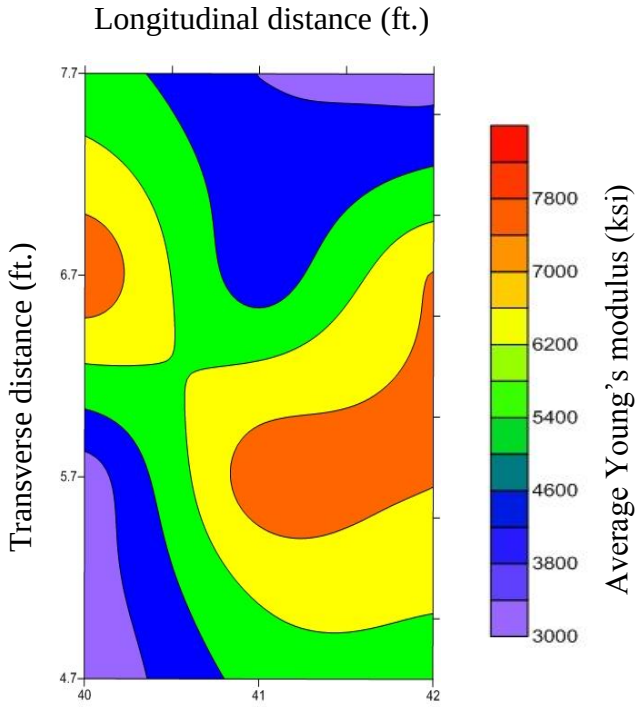

Figure 6.7. Contoured map shows average Young's modulus variations for section (C).

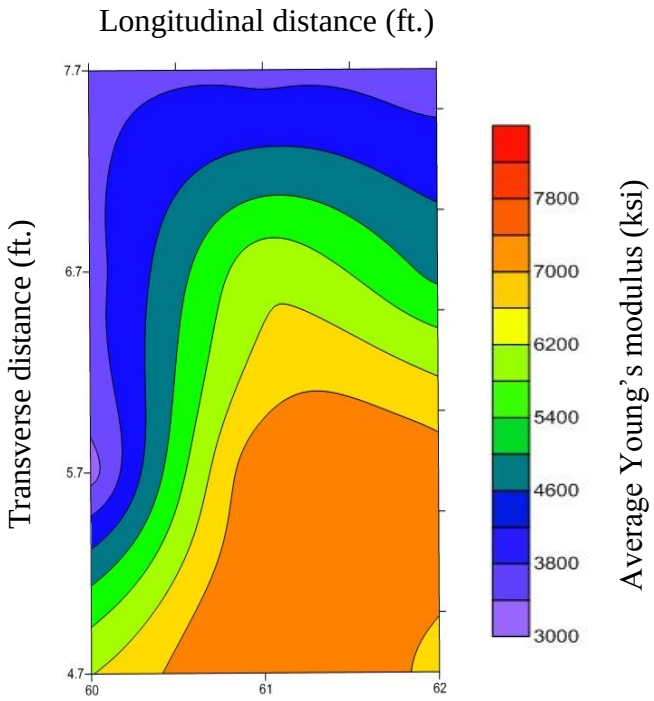

Figure 6.8. Contoured map shows average Young's modulus variations for section (D).

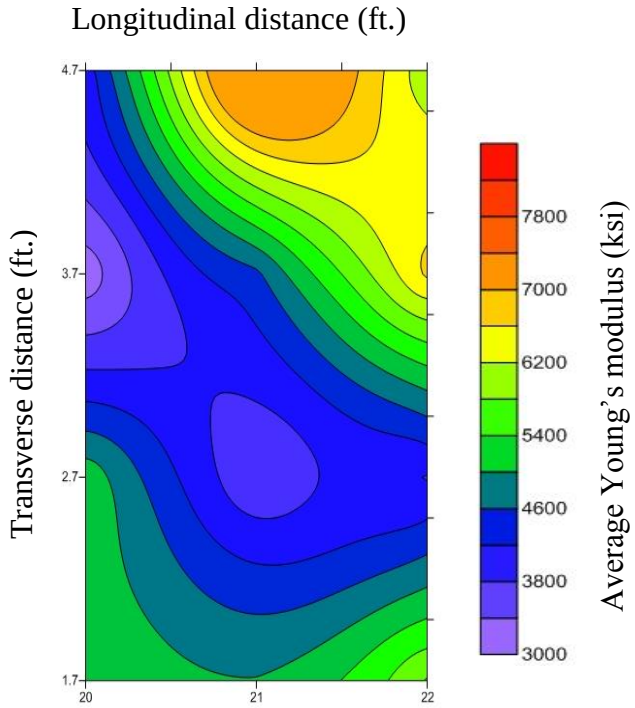

Figure 6.9. Contoured map shows average Young's modulus variations for section (B).

Hammer sounding and chain drag data were qualitatively interpreted. Interpreted data were displayed in a typical view map as shown in (Figure 6.10). The red marked areas corresponding to evidence of delamination (hollow sound) and the remained area of the bridge deck corresponding to no evidence of delamination (solid sound).

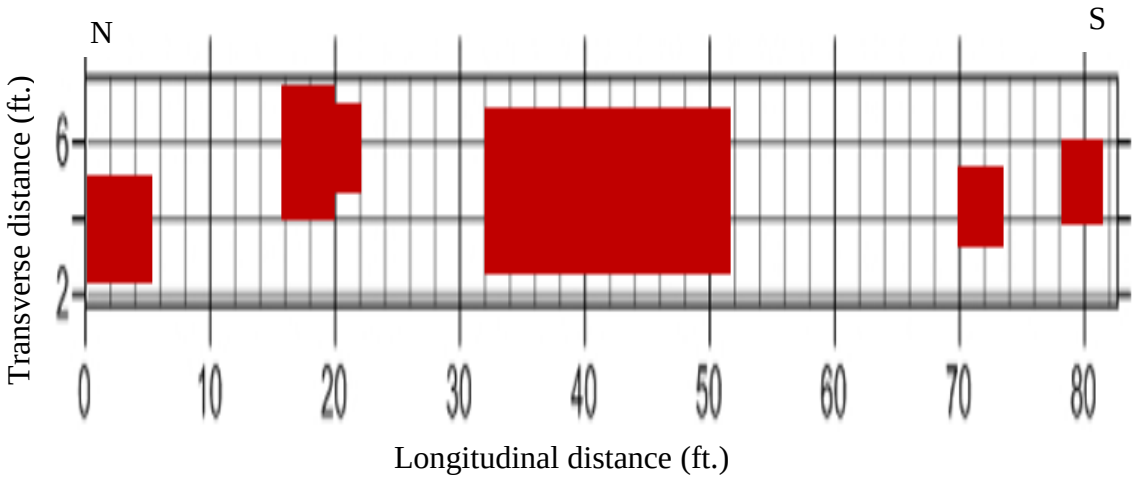

Figure 6.10. View map shows chain drag and hammer sounding data.

The multiple NDTs data were integrated to assess the integrity of the reinforced concrete bridge deck as shown in (Figure 6.11). NDT data were integrated to constrain and verify results of each other.

Visual inspection and GPR data showed a reasonable correlation where the main deteriorated area is located at the center of the bridge deck. However, due to varying depth of reinforcements, GPR cannot be used for bridge deck assessment. Visual inspection, and hammer sounding and chain drag data showed a good correlation especially at the center area of the bridge deck where both indicated evidence of deterioration. GPR and PSPW-USW data were correlated with each other. Section-A showed a poor correlation with the GPR section corresponding with the same grid map as shown in (Figure 6.12). Section-B

and Section-C showed good correlation with the GPR section corresponding with the same grid map as shown in (Figure 6.13) and (Figure. 6.14) respectively. Section-D showed a reasonable correlation with the GPR section corresponding with the same grid map as shown in (Figure 6.15). Section-E showed a poor correlation with the GPR section corresponding with the same grid map as shown in (Figure 6.16).

Visual inspection, GPR, PSPA-USW, and hammer sounding and chain drag data showed a good correlation mainly at center area of the bridge deck where this area is the most deteriorated area of the bridge deck.

6.2. THE EFFECT OF TEMPERATURE AND MOISTURE CONTENT CHANGES ON GPR SIGNAL AMPLITUDE

The GPR signal amplitude was evaluated during different temperature and moisture content changes along the reinforced bridged deck. The increase of temperature and decrease of moisture content creates dryness in the concrete materials in which the concrete have a low dielectric constant. The decrease of temperature and increase of moisture content creates wetness in the concrete materials in which the concrete have a high dielectric constant.

GPR data were acquired during temperature changes of three different temperature change categories: “High temperature” indicated temperature scale in the range of (70-80 °F) as shown in (Figure. 6.17). “Moderate temperature” indicated temperature scale in the range of (50-70 °F) as shown in (Figure. 6.18). “Low temperature” indicated temperature scale less than (50 °F) as shown in (Figure 6.19).

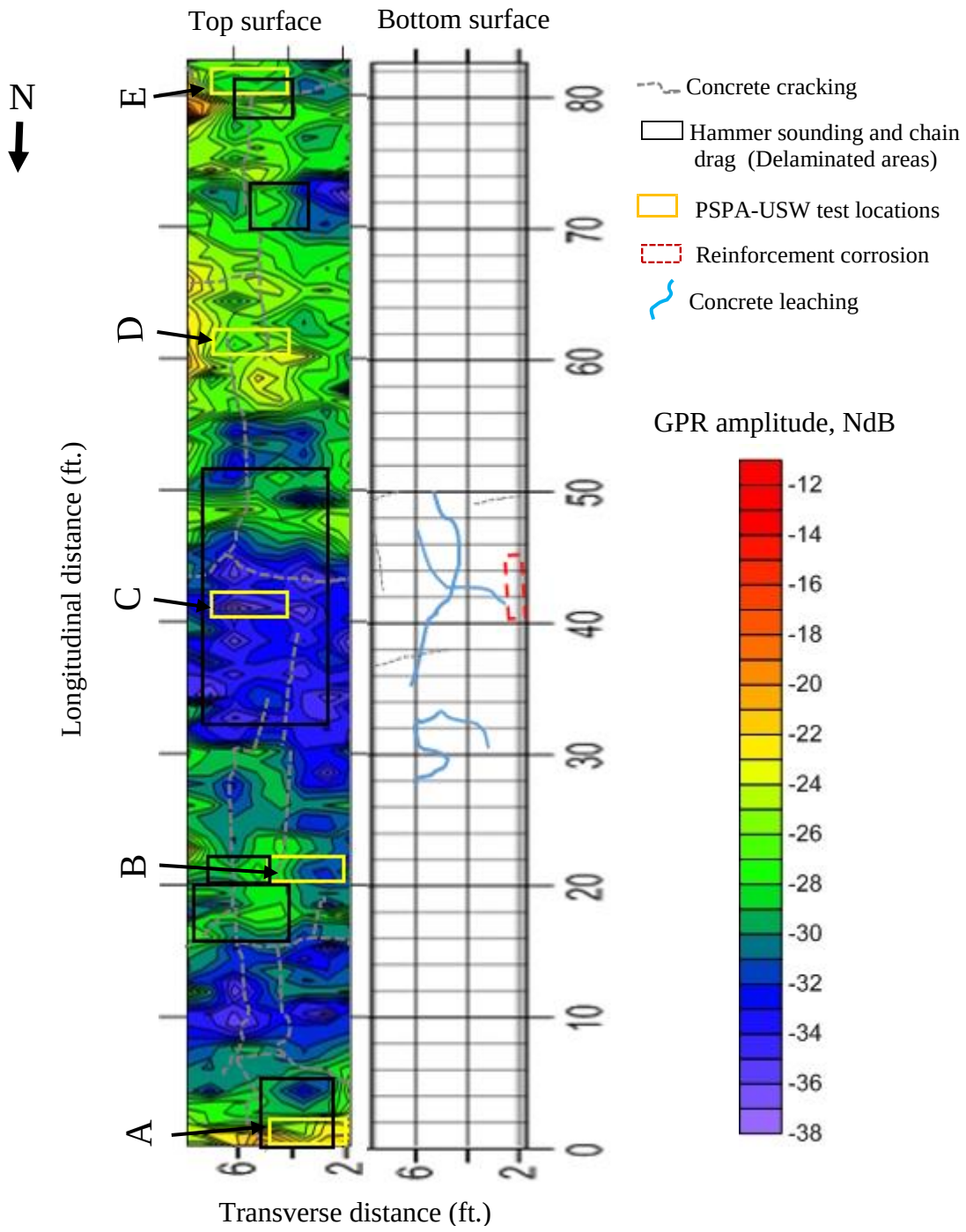

Figure 6.11. Superposed map of visual inspection, GPR, PSPA-USW, and hammer sounding and chain drag data.

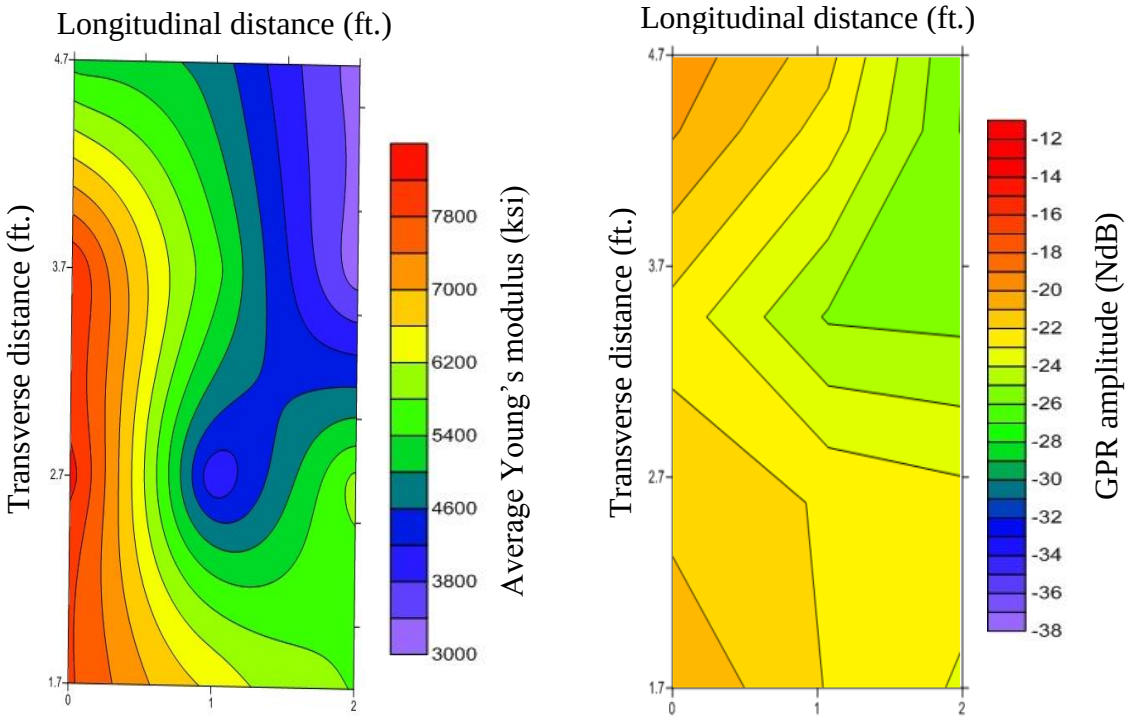

Figure 6.12. PSPA-USW average Young's modulus and GPR amplitude variations for section (A)

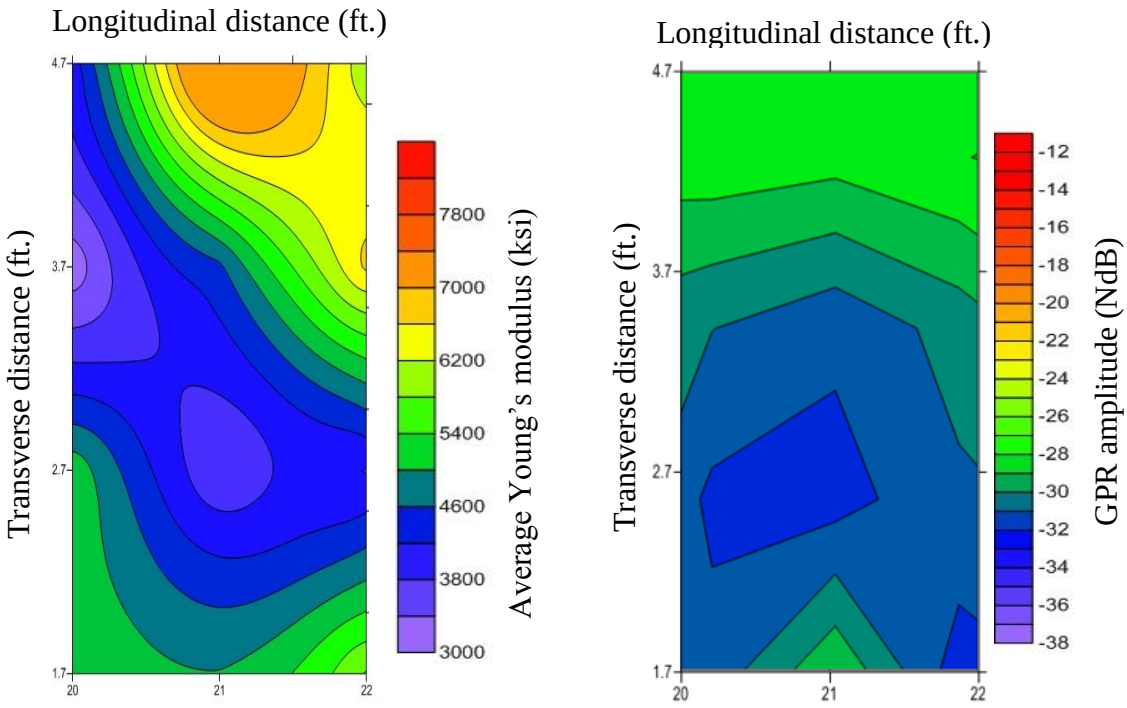

Figure 6.13. PSPA-USW average Young's modulus and GPR amplitude variations for section (B)

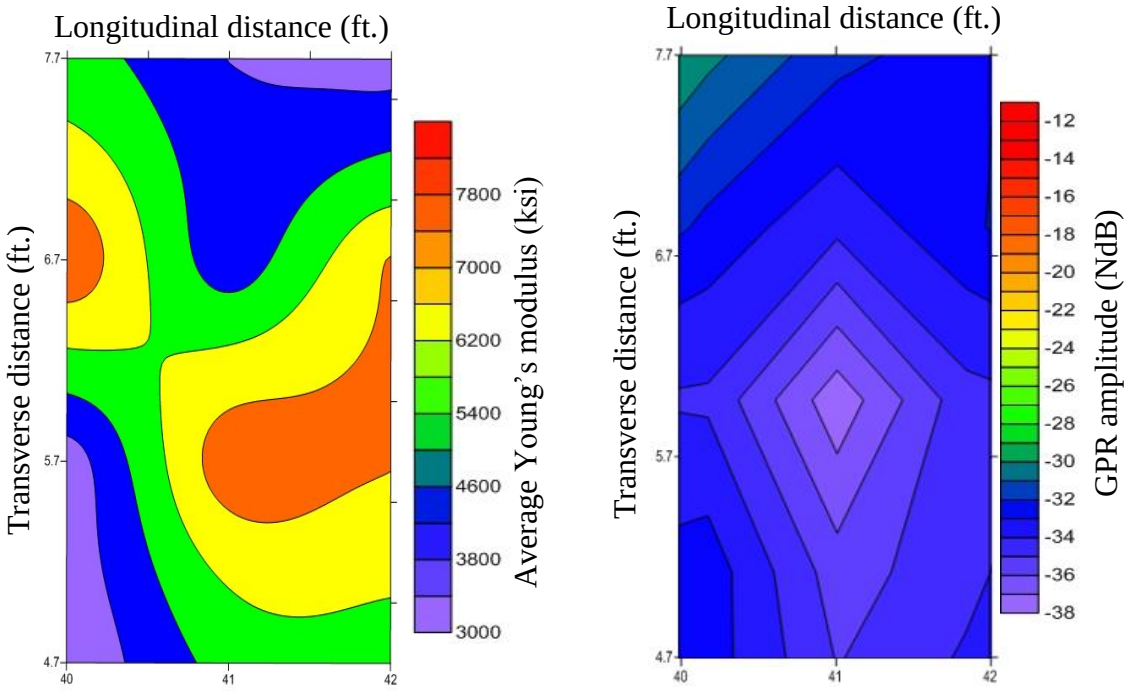

Figure 6.14. PSPA-USW average Young's modulus and GPR amplitude variations for section (C)

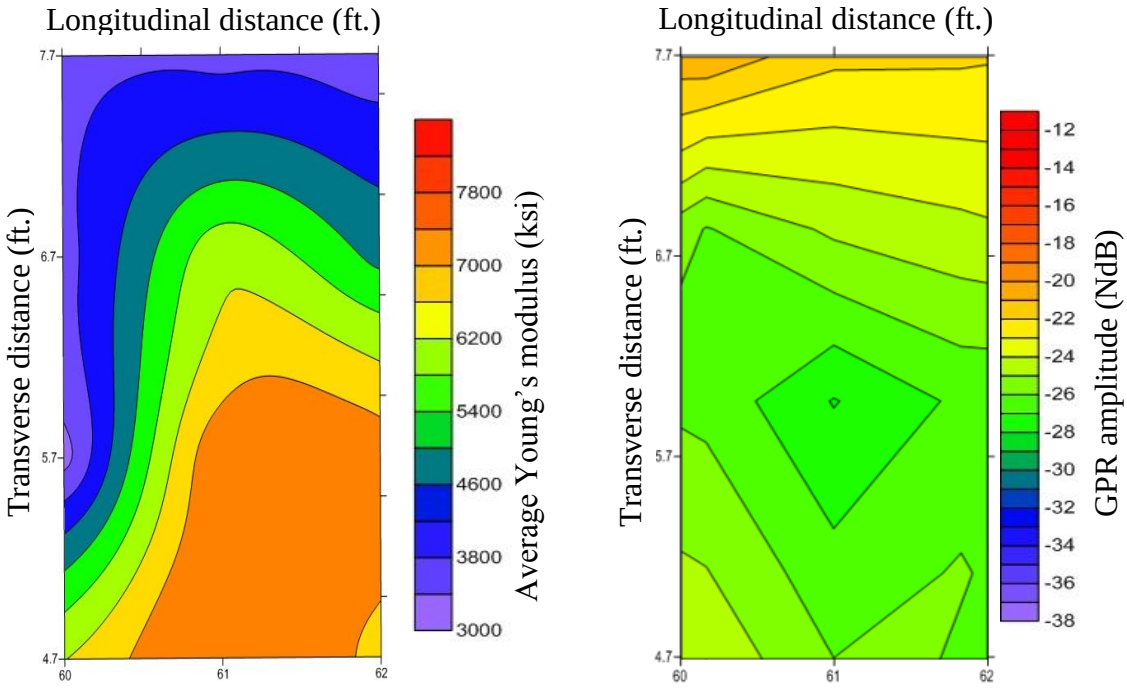

Figure 6.15. PSPA-USW average Young's modulus and GPR amplitude variations for section (D)

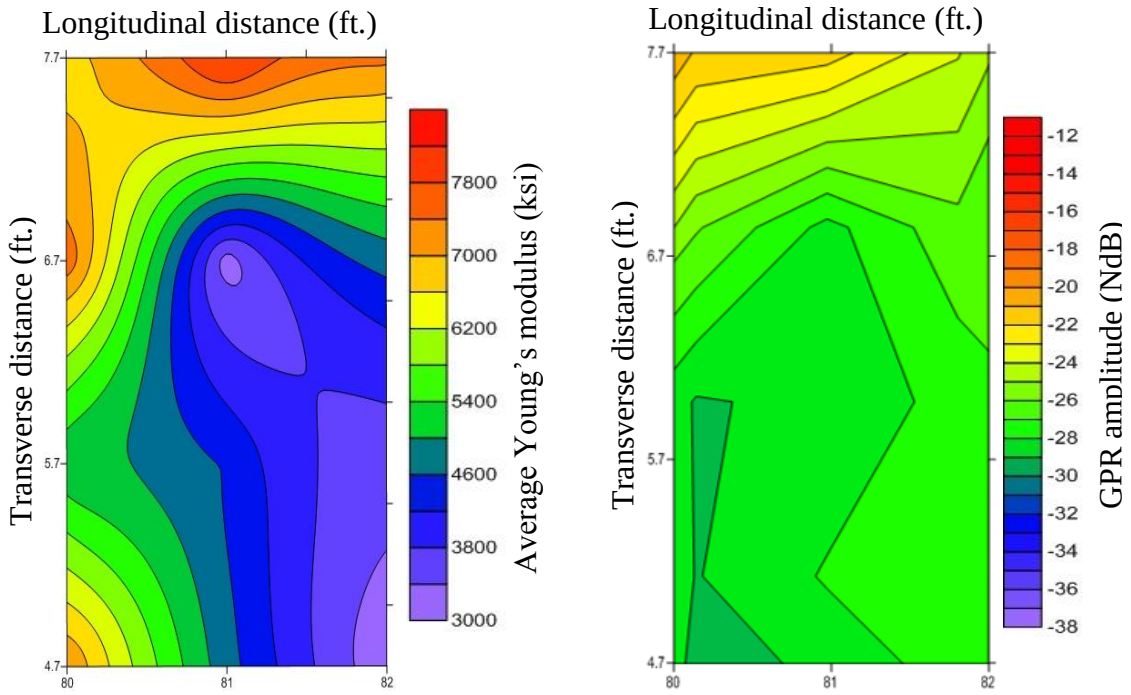

Figure 6.16. PSPA-USW average Young's modulus and GPR amplitude variations for section (E).

GPR signal amplitude maps showed the effect of temperature changes on GPR signal amplitude with stable moisture content of zero (in.) precipitation as shown in (Figures 6.17,6.18,and 6.19). For example, GPR signal amplitude tended to a low attenuation of energy during the high temperature as shown in (Figure. 6.17) where the areas marked with black boxes showed an increase in the amplitude compared with the moderate and low temperature changes effect. GPR signal amplitude tended to a moderate attenuation of energy during the moderate temperature as shown in (Figure. 6.18) the areas marked with black boxes showed a decrease in the amplitude compared with the high temperature changes effect and an increase in the amplitude compared with the low temperature changes effect. GPR signal amplitude tended to a low attenuation of energy during the low temperature as shown in (Figure. 6.19) the areas marked with black boxes

showed an increase in the amplitude compared with the high and moderate temperature changes effect.

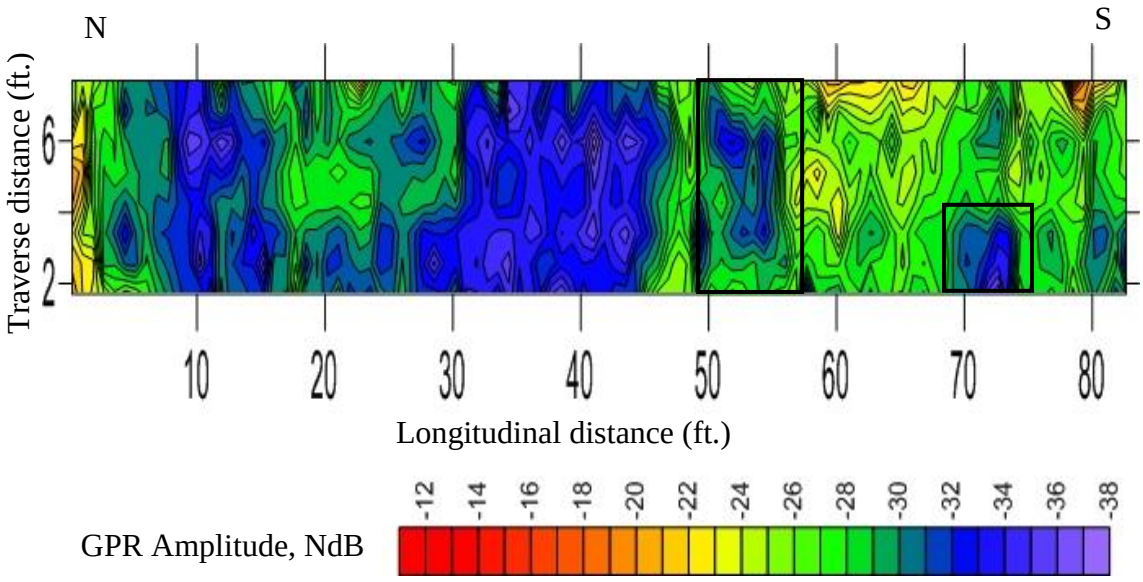

Figure 6.17. GPR amplitude variations map at temperature of 75 (°F) and precipitation of 0.0 (in.).

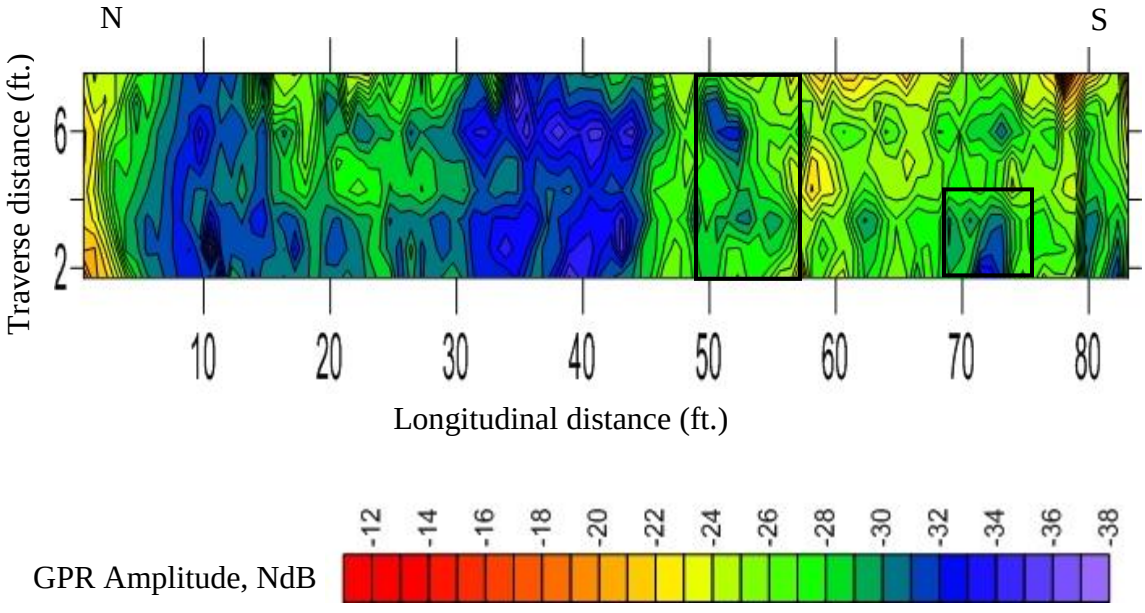

Figure 6.18. GPR amplitude variations map at temperature of 63 (°F) and precipitation of 0.0 (in.).

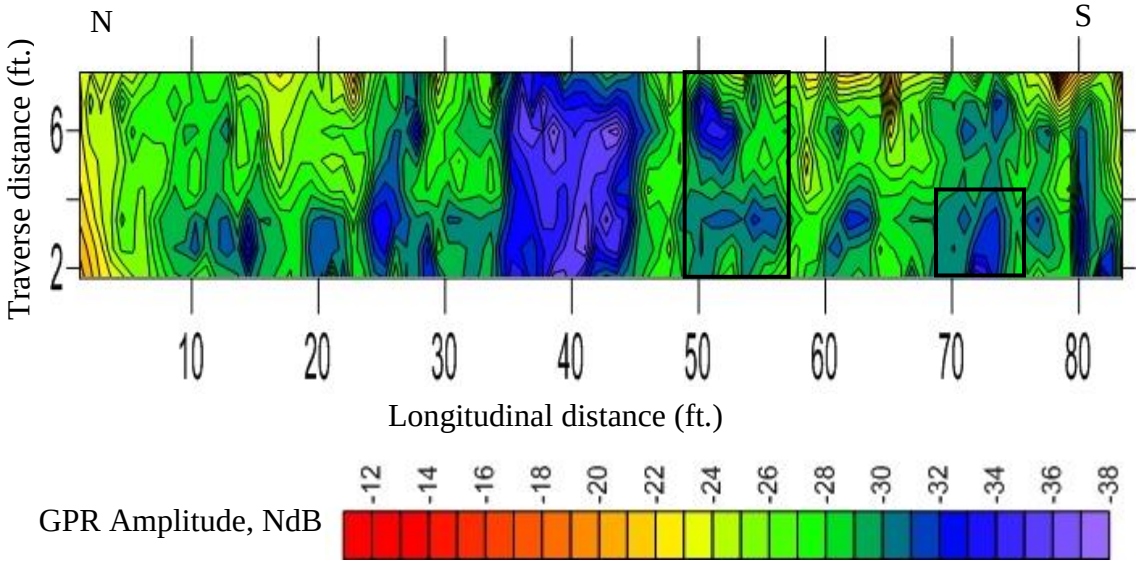

Figure 6.19. GPR amplitude variations map at temperature of 20 (°F) and precipitation of 0.0 (in.).

GPR data were acquired during moisture content changes of three different moisture content change categories: “High moisture content” indicated moisture content of precipitation of 0.7 (in.) as shown in (Figure 6.20). “Low moisture content” indicated moisture content of precipitation of 0.0 (in.) as shown in (Figure 6.21).

GPR signal amplitude maps showed the effect of moisture content changes on GPR signal amplitude with stable temperature of (70 °F) as shown in (Figures 6.20,6.21,and 7.22). For example, GPR signal amplitude tended to a high attenuation of energy during the high moisture content as shown in (Figure. 6.20) the areas marked with black boxes shows an increase in the amplitude compared with the low moisture content change effect. GPR signal amplitude tended to a low attenuation of energy during the low moisture content as shown in (Figure 6.21) the areas marked with black boxes shows a decrease in the amplitude compared with the high moisture content change effect.

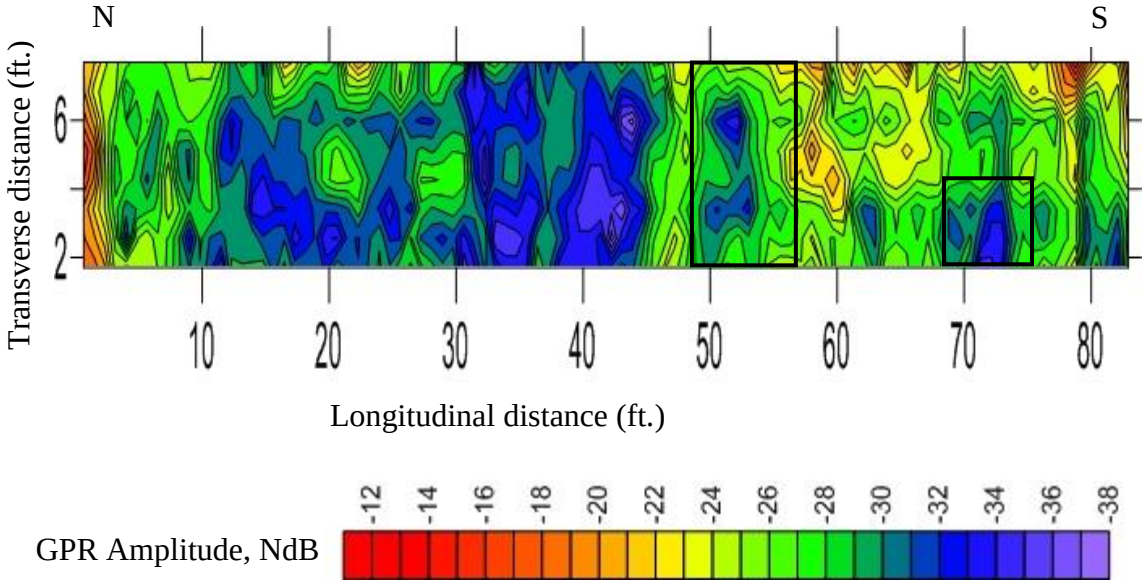

Figure 6.20. GPR amplitude variations map at temperature of 70 (°F) and precipitation of 0.7 (in.).

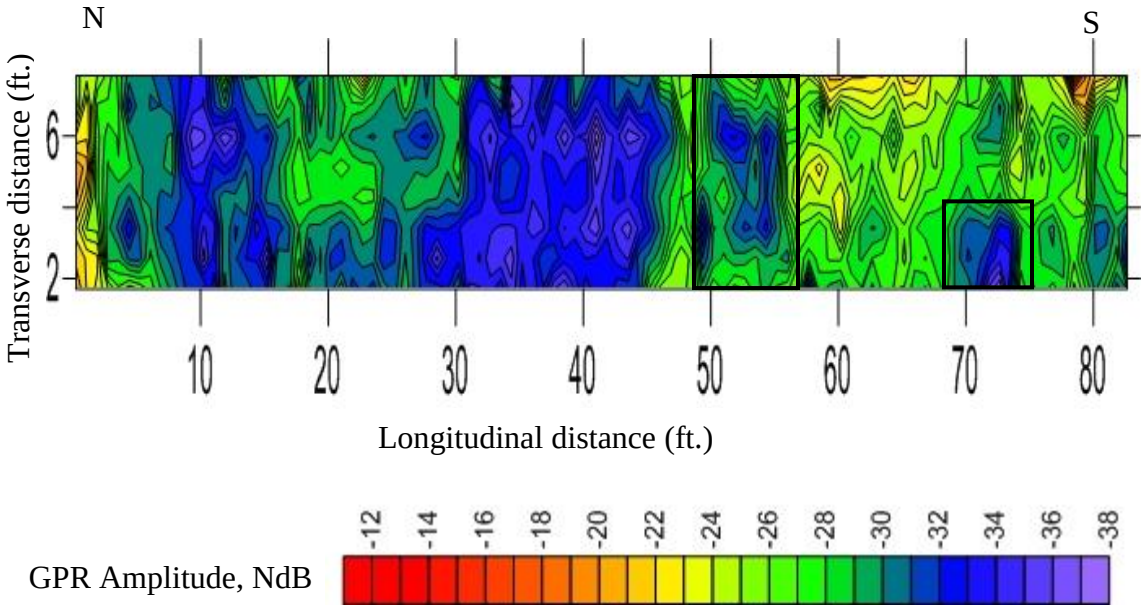

Figure 6.21. GPR amplitude variations map at temperature of 70 (°F) and precipitation of 0.0 (in.).

7. CONCLUSIONS

The complete assessment of reinforced concrete bridge deck requires a complementary approach of using multiple non-destructive techniques. In this study, there were two objectives achieved.

First, non-destructive techniques of visual inspection, ground penetrating radar, portable seismic property analyzer-ultrasonic surface wave, and hammer sounding and chain drag data were used to assess integrity of the bridge deck. Visual inspection data were used to identify signs of deterioration on top and bottom surface of the bridge deck. GPR data were not useful for bridge deck assessment due to the significant varying depth to top of embedded concrete reinforcements. Portable seismic property analyzer-ultrasonic surface wave data were used to determine the concrete quality of the bridge deck by estimating average Young's modulus. Hammer sounding and chain drag data were used to identify the non-delaminated and severe delaminated areas on the bridge deck. There was a good correlation between the employed non-destructive techniques in terms of identifying location of severely deteriorated area mainly at the center of the bridge deck.

Second, GPR signal amplitude variations were evaluated during different temperature and moisture content changes. GPR signal amplitude was increasingly attenuated during low temperature and high moisture content and decreasingly attenuated during high temperature and low moisture content.

BIBLIOGRAPHY

[1] Gucunski, N., & National Research Council. (2013). Nondestructive testing to identify concrete bridge deck deterioration. Transportation Research Board.

[2] Gucunski, N., Romero, F., Kruschwitz, S., Feldmann, R., Abu-Hawash, A., & Dunn, M. (2010). Multiple complementary nondestructive evaluation technologies for condition assessment of concrete bridge decks. Transportation Research Record: Journal of the Transportation Research Board, (2201), 34-44.

[3] El-Safty, A. (2008). Behaviour of RC bridge deck slabs and girders strengthened with CFRP laminates. In Structural Faults and Repair: Proc. 12 th Intern. Conf (pp. 10-12).

[4] Wamweya, A. (2009). Application of ground penetrating radar (GPR) for bridge deck condition assessment: using a 1.5 GHz ground-coupled antenna.

[5] Abudayyeh, O., Abdel-Qader, I., Nabulsi, S., & Weber, J. (2004). Using nondestructive technologies and methods in bridge management systems. Journal of Urban Technology, 11(1), 63-76.

[6] Yehia, S., Abudayyeh, O., Nabulsi, S., & Abdelqader, I. (2007). Detection of common defects in concrete bridge decks using nondestructive evaluation techniques. Journal of Bridge Engineering, 12(2), 215-225.

[7] Anderson, N. (2017). Transportation Applications of Geophysics lectures at Missouri University of Science and Technology.

[8] Li, M. (2017). In-situ assessment of concrete bridge decks and pavements using stress-wave based methods (Doctoral dissertation, Missouri University of Science and Technology).

[9] Ekström, T. (2000). Leaching of concrete: experiments and modelling. Report TVBM (Intern 7000-rapport), 7153.

[10] http://www.fprimec.com/deterioration-of-concrete-structures/\

[11] PCA, T. (2002). Causes of Concrete Deterioration. IS536, Portland Cement Association, Skokie, Illinois.

[12] Gheitasi, A., & Harris, D. K. (2015, June). Performance assessment of steel–concrete composite bridges with subsurface deck deterioration. In Structures (Vol. 2, pp. 8-20). Elsevier.

[13] Sneed, L., Anderson, N., & Torgashov, E. (2014). Nondestructive Evaluation of MODOT Bridge Decks–Pilot Study (No. cmr14-010).

[14] Akhtar, S. (2013). Review of nondestructive testing methods for condition monitoring of concrete structures. Journal of construction engineering, 2013.

[15] Hema, J., Guthrie, W. S., & Fonseca, F. S. (2004). Concrete bridge deck condition assessment and improvement strategies (No. UT-04-16). Brigham Young University, Department of Civil and Environmental Engineering.

[16] Anderson, N., & Li, M. (2014). Testing and Assessment of Portable Seismic Property Analyzer (No. NUTC R297).

[17] Khamzin, A. K. (2015). Advanced approaches for bridge deck assessment using ground penetrating radar.

[18] Barnes, C. L., & Trottier, J. F. (2004). Effectiveness of ground penetrating radar in predicting deck repair quantities. Journal of infrastructure systems, 10(2), 69-76.

[19] Barnes, C. L., Trottier, J. F., & Forgeron, D. (2008). Improved concrete bridge deck evaluation using GPR by accounting for signal depth–amplitude effects. NDT & E International, 41(6), 427-433.

[20] Varnavina, A. V. (2015). Nondestructive and destructive bridge deck condition assessment. Missouri University of Science and Technology.

[21] Cardimona, S., Willeford, B., Wenzlick, J., & Anderson, N. (2001). Bridge Deck Condition Studies in Missouri Utilizing Ground Penetrating Radar (No. RDT01-012,).

[22] Breysse, D., Klysz, G., Dérobert, X., Sirieix, C., & Lataste, J. F. (2008). How to combine several nondestructive techniques for a better assessment of concrete structures. Cement and Concrete Research, 38(6), 783-793.

[23] Annan, A. P., Waller, W. M., Strangway, D. W., Rossiter, J. R., Redman, J. D., & Watts, R. D. (1975). The electromagnetic response of a low-loss, 2-layer, dielectric earth for horizontal electric dipole excitation. Geophysics, 40(2), 285-298.

[24] Maser, K. (2008). Integration of ground penetrating radar and infrared thermography for bridge deck condition testing. Materials Evaluation, 66(11).

[25] Wightman, W., Jalinoos, F., Sirles, P., & Hanna, K. (2004). Application of geophysical methods to highway related problems (No. FHWA-IF-04-021).

[26] McDaniel, M., Celaya, M., & Nazarian, S. (2010). Concrete bridge deck quality mapping with seismic methods: Case study in Texas. Transportation Research Record: Journal of the Transportation Research Board, (2202), 53-60.

[27] Azari, H., Nazarian, S., & Yuan, D. (2014). Assessing sensitivity of impact echo and ultrasonic surface waves methods for nondestructive evaluation of concrete structures. Construction and Building Materials, 71, 384-391.

[28] BAKER, M. R., Crain, K., & Nazarian, S. (1995). Determination of pavement thickness with a new ultrasonic device (No. TX-95 1966-1F).

[29] Bell, H. P. (2006). Operating the Portable Seismic Pavement Analyzer (No. ERDC/GSL-SR-06-9). ENGINEER RESEARCH AND DEVELOPMENT CENTER VICKSBURG MS GEOTECHNICAL AND STRUCTURES LAB.

[30] Federal highway administration research and technology non-destructive evaluation (NDE) Web Manual.

[31] Soutsos, M. N., Bungey, J. H., Millard, S. G., Shaw, M. R., & Patterson, A. (2001). Dielectric properties of concrete and their influence on radar testing. NDT & e International, 34(6), 419-425.

[32] Hubbard, S. S., Zhang, J., Monteiro, P. J., Peterson, J. E., & Rubin, Y. (2003). Experimental detection of reinforcing bar corrosion using nondestructive geophysical techniques. Materials Journal, 100(6), 501-510.

[33] Barnes, C. L., & Trottier, J. F. (2004). Effectiveness of ground penetrating radar in predicting deck repair quantities. Journal of infrastructure systems, 10(2), 69-76. 46

[34] Romero, F. A., Roberts, G. E., & Roberts, R. L. (2000, February). Evaluation of GPR bridge deck survey results used for delineation of removal/maintenance quantity boundaries on asphalt-overlaid, reinforced concrete deck. In Structural Materials Technology IV, an NDT Conf (pp. 23-30).

[35] Barnes, C. L., & Trottier, J. F. (2000). Ground-penetrating radar for network-level concrete deck repair management. Journal of Transportation Engineering, 126(3), 257-262.

[36] Maser, K. R., & Rawson, A. (1992). Network Bridge Deck Surveys Using High-Speed Radar: Case Studies of 44 Decks (Abridgment). Transportation Research Record, (1347).

[37] Laurens, S., Balayssac, J. P., Rhazi, J., & Arliguie, G. (2002). Influence of concrete relative humidity on the amplitude of Ground-Penetrating Radar (GPR) signal. Materials and Structures, 35(4), 198-203.

[38] Kodi, A. (2016). Imaging reinforced concrete: A comparative study of ground penetration radar and Rebarscope. Missouri University of Science and Technology.

VITA

Abdullah Hadi Zaid Alhaj was born in Yemen. He completed his high school at Mukalla Model Secondary School in 2010 with excellence. Then he received a fully scholarship to pursue his undergraduate degree at King Saud University in Saudi Arabia. He received his B.S. of applied geophysics in 2015 with the first class honor. Then he worked as geophysical engineer at explorer for geophysical consultations. Afterwards, he received a fully scholarship from Hadhramout Establishment for Human Development (HEHD) to pursue his M.S. In December 2018, he received his M.S degree in Geological Engineering from Missouri University of Science and Technology. During his graduate school, he has been involved in multiple funded projects including ground penetrating radar (GPR), electrical seismic tomography (ERT), seismic refraction (SR) and electromagnetic (EM) methods. In addition, he published two research papers as a first author and three research papers as a second co-author. He participated with some conference papers in national and international conferences. He was a member of society of exploration geophysicists (SEG), american geophysical union (AGU), geological society of america (GSA), and society of petroleum engineers (SPE).